processes

MDPI

Review

A Comprehensive Review of Organic Rankine Cycles

José C. Jiménez-García, Alexis Ruiz, Alejandro Pacheco-Reyes and Wilfrido Rivera *

Instituto de Energías Renovables, Universidad Nacional Autónoma de México, Temixco 62580, Mexico; jcjig@ier.unam.mx (J.C.J.-G.); asrual@ier.unam.mx (A.R.); parea@ier.unam.mx (A.P.-R.)
* Correspondence: wrgf@ier.unam.mx; Tel.: +52-77-7362-0090 (ext. 29740)

Abstract: It has been demonstrated that energy systems driven by conventional energy sources like fossil fuels are one of the main causes of climate change. Organic Rankine cycles can help to reduce that impact, as they can be operated by using the industrial waste heat of renewable energies. The present study presents a comprehensive bibliographic review of organic Rankine cycles. The study not only actualizes previous reviews that mainly focused on basic cycles operating on subcritical or supercritical conditions, but also includes the analysis of novel cycles such as two-stage and hybrid cycles and the used fluids. Recuperative and regenerative cycles are more efficient than reheated and basic single-stage cycles. The use of two-stage cycles makes it possible to achieve higher thermal efficiencies and net power outputs of up to 20% and 44%, respectively, compared with those obtained with single-stage cycles. Theoretical studies show that hybrid systems, including Brayton and organic Rankine cycles, are the most efficient; however, they require very high temperatures to operate. Most organic Rankine cycle plants produce net power outputs from 1 kW up to several tens of kW, mainly using microturbines and plate heat exchangers.

Keywords: microturbines; organic Rankine cycles; polygeneration; power production; waste heat recovery

Citation: Jiménez-García, J.C.; Ruiz, A.; Pacheco-Reyes, A.; Rivera, W. A Comprehensive Review of Organic Rankine Cycles. *Processes* **2023**, *11*, 1982. https://doi.org/10.3390/pr11071982

Academic Editor: Ambra Giovannelli

Received: 10 May 2023
Revised: 5 June 2023
Accepted: 28 June 2023
Published: 30 June 2023

1. Introduction

Climate change is a huge problem that humanity is facing, due to carbon dioxide (CO_2) emissions into the atmosphere due to the consumption of fossil fuels. According to the International Energy Agency (IEA), in 2021, 36.3 gigatons of CO_2 were released into the environment [1]. According to the U.S. Department of Energy [2], in that country alone, the potential of unrecovered waste heat at temperatures below 150 °C is about 75×10^9 kW/year, with the largest waste heat sources being the exhaust gases from burners, furnaces, dryers, heaters, and heat exchangers [3]. Many studies have been carried out on the development of organic Rankine cycles (ORCs). Unlike Rankine cycles, ORCs utilize an organic fluid instead of steam, and their capacities are considerably lower. Moreover, the operating temperatures generally do not exceed 150; hence, they are applied to recover waste heat or to take advantage of renewable energies.

In recent years, some reviews of works looking at ORCs were carried out. Park et al. [4] reported a review focusing on experimental ORC performance. The authors analyzed and reported the most relevant data on prototypes, systems developed, and trends. Tartière and Astolfi [5] analyzed the market evolution and its applications, mainly focusing on waste heat recovery. They also analyzed the future perspectives and market growth potential. Pethurajan et al. [6] carried out a bibliographic review on the selection of the turbine for ORCs, and its applications when used as topping or bottoming cycles. On the other hand, Ahmadi et al. [7] and Haghighi et al. [8] carried out bibliographic reviews of geothermal ORCs. Both papers focused on the analysis of a basic ORC, an ORC with a recuperator, and a regenerative ORC for electricity production. The paper published by Haghighi et al. [8] focused mainly on the modeling and optimization of ORCs using a considerable number of different working fluids and reporting values of energy and

exergy efficiencies, while the paper published by Ahmadi et al. [7] additionally analyzed economic indexes such as the electricity production cost and the levelized cost of electricity; besides this, they compared the results with other conventional power generation systems. Moreover, Wieland et al. [9], also presented the recent advances and future perspectives for ORCs from the market perspective. Although these bibliographic reviews include different topics, they mainly focused on basic ORCs.

To date, in the literature, there are a large number of studies focused on the thermodynamic optimization of ORC and the development of new cycles trying to develop more efficient technologies. The purpose of the present review work is to summarize and classify what is considered the most outstanding studies that, through multiple and diverse strategies, have proposed and analyzed new key configurations addressed to improve the performance and to adapt the organic cycles to satisfy the current and very varied energy needs. The present bibliographic review not only updates the state of the art of basic ORCs operating on subcritical or supercritical conditions (as was generally done in previous reviews), but also includes the analysis of novel ORCs such as two-stage, hybrid, and polygeneration systems composed of ORC and one or more different technologies to handle at least two different outputs. The analysis includes systems driven by geothermal energy, solar energy, and waste heat recovery produced from engines or industrial processes. Moreover, this bibliographic review also includes an analysis of the different working fluids used in the different types of ORCs.

This document is structured as follows: the second section describes the basic ORC, its main modifications, and the primary substances utilized as working fluids. Section 3 presents the bibliographic review of single-stage systems, including their thermo-economic and life cycle analysis. This section includes the most outstanding experimental research in this field. Section 4 describes the cycle configurations of recuperative, regenerative, and reheated ORCs and a comparison of them, as well as the advantages they offer in terms of energy. This section also describes the supercritical cycles. Section 5 is related to novel designs of a two-stage ORC, in which at least two heat supplies are driving the system. Section 6 summarizes the hybrid cycles, which are cycles in which an ORC is integrated as a topping or bottoming cycle to increase the power production or energy/exergy efficiency. Finally, in Section 7 the future directions of the research on ORCs are also addressed.

2. Description of Organic Rankine Cycles

A basic ORC consists of four main components: an evaporator, an expander, a condenser, and a pump. Figure 1 shows the simplest ORC configuration. As can be seen, liquid in saturated conditions (1) is pumped, increasing its pressure, into the evaporator (2) where it is evaporated by supplying energy in the form of heat. Then, the working fluid leaving the evaporator (3) enters the expander, reducing its pressure (4) while producing power. Then, the fluid passes to the condenser, where it is liquefied (1), repeating the cycle. This ORC is sometimes called a single-pressure or single-stage ORC, because it uses only one evaporator.

To reduce the heat supplied to the evaporator and increase the efficiency of the system, heat exchangers can be added to the basic cycle. Some of the most well-known ORC configurations are the recuperative, the regenerative, and the reheated cycles.

Figures 2 and 3 show schematic and T-s diagrams of a recuperative and a regenerative ORC, respectively. Both cycles attempt to reduce the heat supplied to the evaporator, increasing the system's efficiency. In the recuperative cycle, an extra heat exchanger called a "recuperator" is used to preheat the working fluid going to the evaporator to reduce the heat load, while in the regenerative ORC, a working fluid bleed is made at an intermediate pressure on the expander, which is mixed in an open heat exchanger, sometimes called a regenerative tank, to preheat the working fluid coming from the condenser.

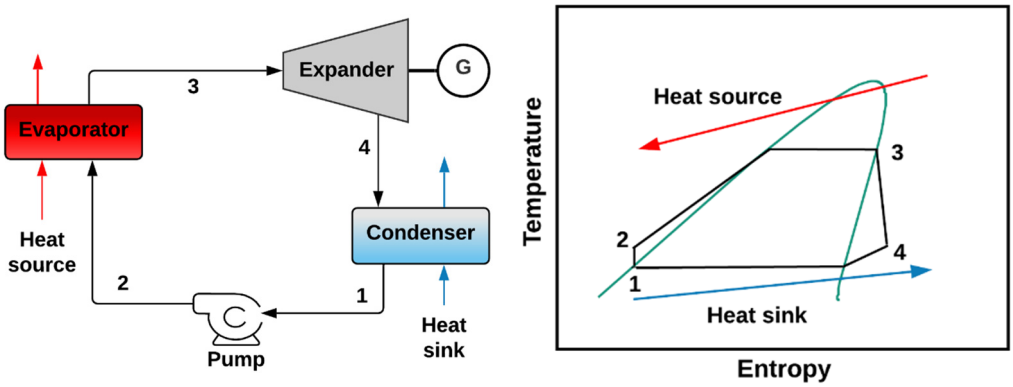

Figure 1. Basic ORC (**a**) Schematic diagram; (**b**) T-s diagram (arrows here represent the energy and entropy changes for the heat source and sink).

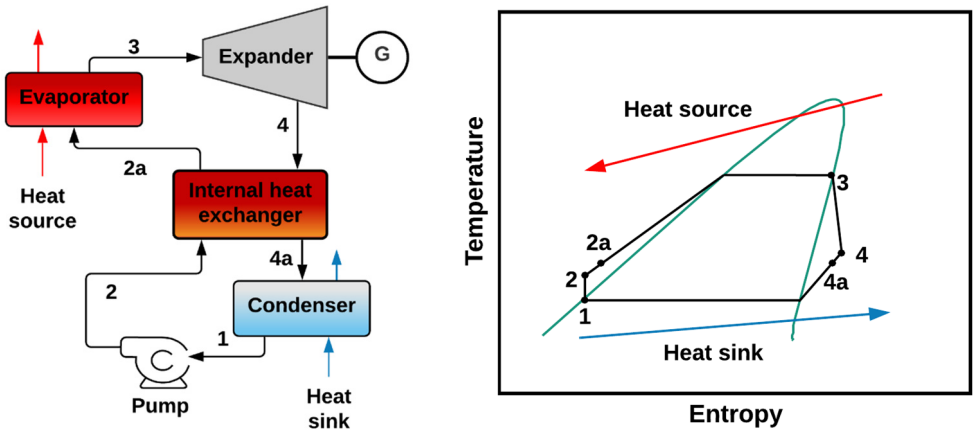

Figure 2. Recuperative ORC (**a**) Schematic diagram; (**b**) T-s diagram.

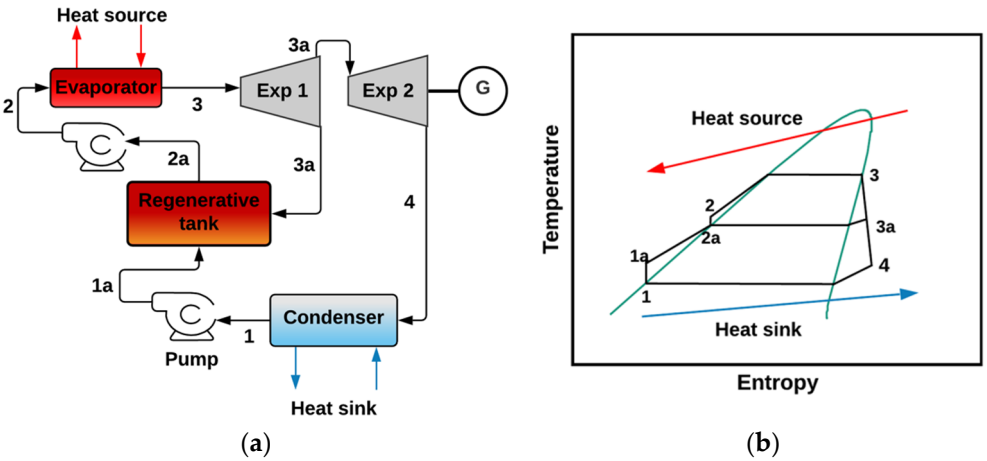

Figure 3. Regenerative ORC (**a**) Schematic diagram; (**b**) T-s diagram.

In a similar way to the regenerative cycle, in the reheated ORC, a bleed of the working fluid is made at an intermediate pressure, but instead of using an additional heat exchanger to preheat the liquid before entering the evaporator, the superheated working fluid is reheated in the evaporator before entering the second expander, as can be seen in Figure 4. In this case, the purpose of the modification is not to decrease the heat supplied to the evaporator, but to increase the system efficiency by increasing the power production.

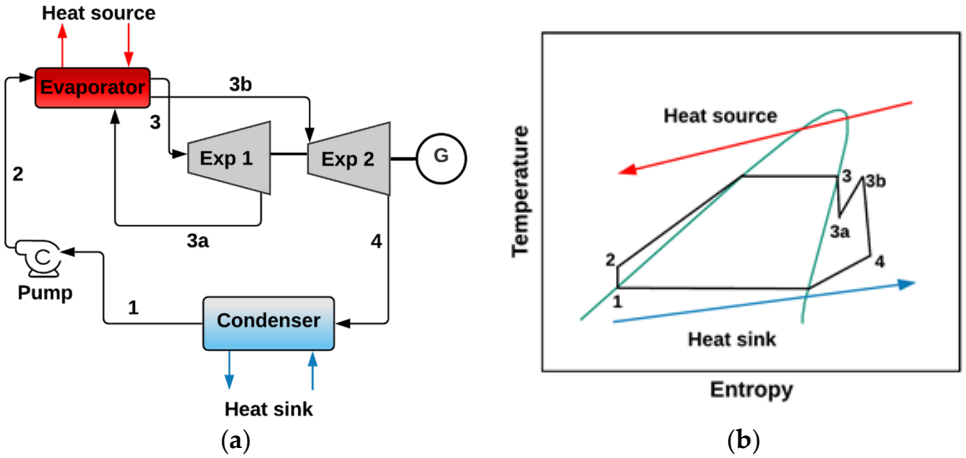

Figure 4. Reheated ORC (**a**) Schematic diagram; (**b**) T-s diagram.

Another configuration of interest to be analyzed is the combination of a recuperative and a regenerative cycle, which offers the advantages of both cycles previously described. This configuration is shown in Figure 5.

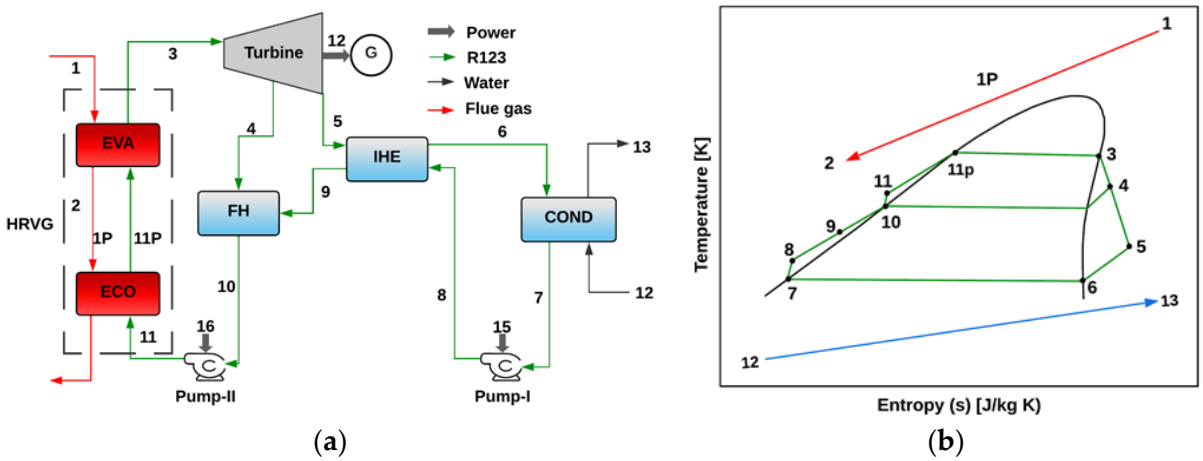

Figure 5. Recuperative–regenerative ORC (**a**) Schematic diagram; (**b**) T-s diagram. Figure modified from Nondy and Gogoi [10].

Working Fluids for ORC

Although most of the previous papers compared the performance of the basic ORC using different working fluids, there are some studies aiming to find the best working fluids from the thermodynamic point of view. Zhang et al. [11] studied fifty-seven fluids based on their saturated vapor curves and classified them as wet, dry, and isentropic, as shown in Figure 6. It was found that the triangle area formed by the critical point and the saturated conditions at the turning point has an important effect on the system performance. The best performance was achieved with fluids with turning points above 200 °C and triangle areas below 6 kJ/kg. The R123 was the best fluid at temperatures lower than 130 °C, achieving a value of 17.5%. At temperatures between 130 °C and 230 °C, the highest efficiencies were obtained with hexane, R113, and isobutane, reaching efficiencies of 22%, 21.5%, and 20%, respectively, and at temperatures around 330 °C, toluene and benzene were the best working fluids, achieving efficiencies of 29% and 28.5%, respectively.

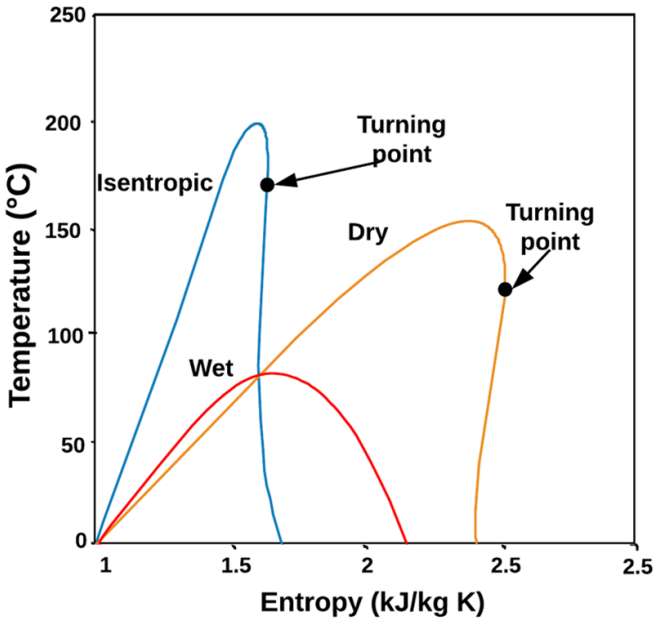

Figure 6. Saturated vapor curves for wet (red), dry (orange), and isentropic (blue) working fluids.

Györke et al. [12] and Imre et al. [13] proposed a new method to determine the best working fluids for low-temperature applications. The method was based on the development of a correlation related to the molar isochoric specific heat capacity of saturated vapor states. They concluded that if the molar isochoric heat capacity of the saturated vapor phase of a fluid was smaller than 80 J/(mol·K) at a temperature 0.74 times the critical temperature, then the fluid was most likely a wet fluid, but if the heat capacity values were higher than this limit, the fluids were most likely dry or isentropic. Györke et al. [14] proposed a new classification to determine the best fluids considering different thermodynamic characteristics such as the possibility of achieving total evaporation by adiabatic expansion or ending in a two-phase state. With these considerations, the authors proposed eight novel fluid categories instead of just three, as proposed by Zhang et al. [11]. In the search for the best working fluid, Wang et al. [15] proposed a method to select a zeotropic mixture for ORC with varying heat source temperatures, i.e., when the ORC is used as a bottoming cycle in a hybrid configuration. The authors found that, for temperatures around 225 °C, the zeotropic mixtures benzene/m-xylene and cyclopentane/toluene obtained the highest performance. Regarding the proposed method, it was found that it was more effective when the heat source temperature varied together with the ambient temperature, because the net power and exergy efficiency improved up to 22% in winter, but that enhancement was just 6.8% in summer. Blondel et al. [16] also studied the use of zeotropic mixtures (Novec649 and HFE7000) as working fluids in ORCs. The authors proposed some two-phase semi-empirical heat transfer correlations (in evaporation and condensation) and evaluated the influence of the heat sources (at high and low temperatures) on the cycle performance. The authors found that zeotropic mixtures of HFE type with low glide values do not favor a better performance than that of the pure fluids.

Yang et al. [17] presented a study of the relationship between critical and boiling temperatures for more than 250 working fluids. The results showed that at temperatures between 150 °C and 200 °C, the strong relationship between the maximum net power and the critical temperature was not affected by the reduced boiling temperature. However, at temperatures between 250 °C and 300 °C, working fluids with reduced boiling temperatures higher than 0.7 exhibited maximum net power even at optimum critical temperatures. Li et al. [18] determined the best fluid based on a parameter defined as equivalent hot-side temperature. This parameter was obtained as the ratio of the isentropic fluid expansion to the entropy change of the whole cycle. For more than half of the working fluids, the relative error was within ±0.6%. Dai et al. [19] performed a study using diverse

hydrocarbons operating at four different heat sources. The propyne, cis-butene, iso-hexane, and cyclohexane achieved the highest energy efficiencies, with values of 12.12%, 16.58%, 19.16%, and 21.43% driven by geothermal energy, solar energy, engine waste heat energy, and high-temperature solar energy, respectively. [20]

Fan et al. [21] proposed a method to directly correlate some working fluid properties with the performance of an ORC. This method, based on the fluid's thermal properties, represents a more adequate criterion for the selection of the appropriate working fluid in an ORC, and represents a better alternative to the limited selection criterion based only on the critical temperature. Moreover, the proposed method allows the identification of the applicable range of different types of working fluids as a function of the heat source temperature. On the other hand, Zhang and Li [22] studied the super-dry working fluids used in regenerative ORCs for medium and low heat-source temperatures. According to the authors, distinguishing between a "super-dry fluid" and a "dry fluid" can be carried out through the area of a curved triangle in the zone of superheated vapor in a temperature–entropy diagram: a super-dry fluid has an area greater than 25 kJ/kg, while a dry fluid has an area between 5 kJ/kg and 25 kJ/kg.

Some researchers have assessed the working fluids' environmental impact, such as the case of Bianchi et al. [23], who estimated the greenhouse effect of two pure fluids and four mixtures used to replace the HFCs in organic Rankine systems on the scale of kW. The method utilized considers direct and indirect emissions. The authors validated their model with experimental data, and found that indirect emissions of hydrofluoroolefins may lead to higher CO_2 emissions in the case of the use of R134a as the working fluid. Since parameters like emission factors, fluid leakage rate, and R134a concentration can significantly affect the environmental evaluation, the authors also analyzed and discussed them. A complete review of low global warming potential (GWP) working fluids in ORC applications is presented by Bahrami et al. [24]. This study presented some methodologies for the working fluid selection, and as alternative fluids such as hydrocarbons, hydrofluorochemicals, and mixtures, are included there as well.

3. Single-Stage ORC

As previously mentioned, there are different configurations of single-stage ORCs, and all of them have been analyzed from different points of view by diverse authors. Therefore, the present section has been divided accordingly, with respect to each of these configurations. Additionally, this section includes some studies regarding supercritical ORCs.

Nurhilal et al. [25] modeled a geothermal organic Rankine cycle (G-ORC) using R601. At a temperature of 165 °C, the energy efficiency was 14.61%. Herath et al. [26] performed a similar study, but using other fluids. The best efficiency (18.5%) was achieved with benzene at 194 °C. That efficiency was higher than the one reported by Nurhilal et al. [25], but required higher temperatures. Yadav and Sircar [27] modeled a similar system, but using R600, R600a, R134a, and R245fa. The highest efficiency of 8% was achieved using R134a. Wang et al. [28] modeled an ORC using the hydrofluoroethers at temperatures varying from 67 °C to 112 °C. The highest energy and exergy efficiencies were 12.2% and 52%, respectively, using HFE700.

Sakhrieha et al. [29] modeled an ORC driven with solar and geothermal energies at 60 °C in Jordan. From sixteen working fluids, it was found that the R600, R32, R290, and R410a were the best. Acar and Arslan [30] performed a similar analysis using R600a, but included a storage tank. The energy and exergy efficiencies decreased with the integration of solar energy. The maximum energy and exergy efficiencies were 14.56% and 71%, respectively. Bademlioglu [31] carried out the exergy analysis of a G-ORC using R123, R152a, R245fa, and R600a. The best working fluid was R123, achieving a maximum exergy efficiency of 57%. Yamankaradeniz et al. [32] analyzed the variation in the evaporator effectiveness in a G-ORC, and found that the energy and exergy efficiencies increased up to 6.87% and 6.21%, with the increment of the effectiveness.

Invernizzi et al. [33] studied a modified ORC including a flashing tank and a mixing chamber, as shown in Figure 7. It was found that the use of water/organic fluid mixtures was convenient in terms of system performance and turbine design.

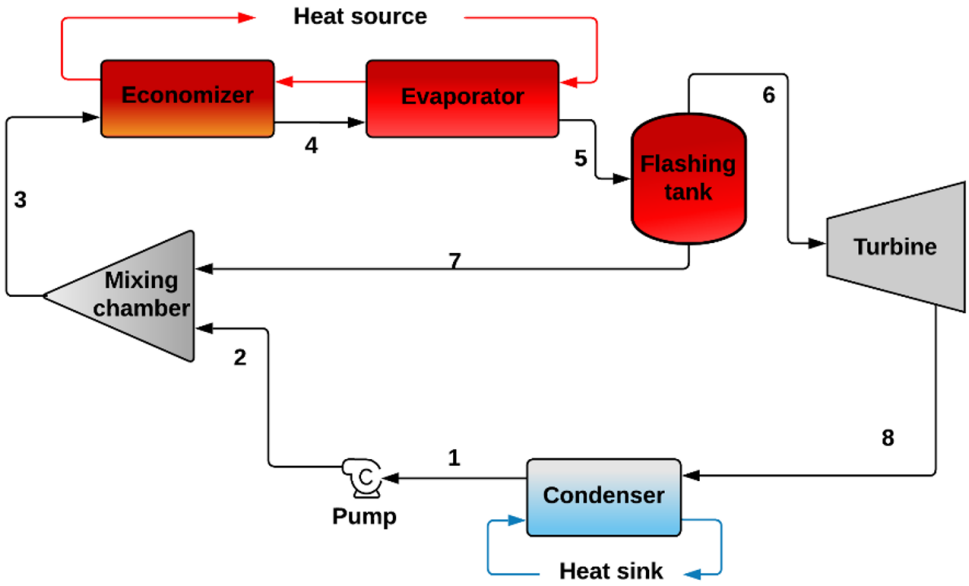

Figure 7. Thermodynamic ORC using a flashing tank and a mixing chamber, proposed by Invernizzi et al. [33]. Colorful arrows represent the heat flow from the heat source (red arrow) to the system, and from the system to the heat sink (blue arrow).

On the other hand, Sun et al. [34] proposed improving the performance of a basic ORC through the implementation of a vacuum condensation process. The results showed that, for some working fluids, the exergy efficiency of the cycle was increased by almost 8% just by reducing the condensation pressure from 0.1 to 0.001 MPa; however, some other working fluids had different optimal condensation pressures, and the cycle efficiencies began to decrease when the pressures approached 0.001 MPa.

Some studies have focused on the implementation of ORC to improve the performance of other systems, like internal combustion engines. Such is the case of Neto et al. [35], who proposed using an ORC coupled to a stationary diesel engine to take advantage of the exhaust gases of the latter to produce power. The study focused on parametric and economic analyses for determining the optimal operating point from these perspectives. It was found the proposed configuration increases the power produced and the thermal efficiency while reducing fuel consumption, and thus, the system's contribution to pollution. Another study on the integration of an ORC and an internal combustion engine was carried out by Ping et al. [36]. The authors proposed a model to assess and optimize the performance of the coupled system under different complex driving cycles. Some parameters, such as the speed of the expander and pump in the ORC, as well as the exhaust valve timing and the change of the cooling water temperature in the internal combustion engine, directly affect the system's performance parameters. According to the results, another key parameter affecting the system performance under dynamic conditions is vehicle speed.

3.1. Thermoeconomic and Life Cycle Analysis of ORC

Other studies have focused on the thermoeconomic analysis of ORCs. Khosravi et al. [37] reported the levelized cost of energy (LCOE) for an ORC operating with nine different working fluids, finding that a minimum LCOE of 0.099 USD/kWh was obtained by using R1234yF. Dai et al. [19] performed a similar study, but using hydrocarbons. The lowest energy costs were determined for propyne, pentane, cyclohexane, and cyclohexane, which were 1.46 USD/kWh, 1.28 USD/kWh, 1.05 USD/kWh, and 0.95 USD/kWh, respec-

tively. Sun et al. [38] carried out a thermoeconomic evaluation, varying the evaporator pinch point temperature difference. It was found that a lower pinch point temperature difference causes a higher turbine output but increases the heat transfer area required by the heat exchangers, as well as the investment costs. At 150 °C the payback period (PBP) of just the ORC was about 4 years, while at 100 °C, the PBP was 8.9 years. If a drilling cost of 500 USD/m was added to the total system costs, the PBP varied from 5.26 to 12.86 years. Mustapić et al. [39] analyzed a geothermal ORC (G-ORC) in the city of Karlovac, Croatia, using diverse fluids. The authors reported a net power index, which is the inverse of the electricity production cost. The lowest values were 0.3361W/EUR (0.397 W/USD) and 0.3375 W/EUR (0.398 W/USD) using n-pentane and isopentane, respectively. Kyriakarakos et al. [40] reported a similar study, but on the Greek island of Milo, and compared their results with other renewable technologies. It was found that the geothermal ORC had a better performance than configurations using solar photovoltaic and wind turbines.

Usman et al. [41] performed a study of a G-ORC cooled by air and by using a cooling tower operating with R245fa and R1233zde. It was found that the R1233zde had the potential to replace the R245fa at temperatures higher than 145 °C. The ORCs using cooling towers were a better alternative for dry and hot climates, while the systems cooled by air could be a better alternative for cold and humid weather. Oyewunmi and Markides [42] performed a thermoeconomic study operating with seven different zeotropic mixtures and compared the results to those achieved using pure working fluids. Although by using the zeotropic mixtures higher efficiencies were reached, the system operating costs with pure n-pentane and R245fa were 14% lower. Yaïci et al. [43] analyzed a solar ORC operating with twelve zeotropic mixtures. The highest efficiencies were obtained using mixtures involving R245fa. The R245fa/propane mixture had the highest sustainability index, with a minimum cost of electricity of 0.15 USD/kWh. Baral [44] modeled an ORC installed in Nepal, driven with geothermal and solar energies using R134a and R245fa. It was found that the LCOE was 0.17 USD/kWh with R134a and 0.14 USD/kWh with R245fa. Ergun et al. [45] carried out an exergoeconomic study of a G-ORC in Turkey. The lowest electricity production cost was 7.96 USD/GJ (0.0287 USD/kWh).

Oyekale et al. [46] performed an exergoeconomic assessment of a hybrid ORC cogeneration plant, using solar energy and biomass. The economic performance was assessed at a component level using the conventional specific exergy costing approach. The criteria for the exergoeconomic evaluation were the exergy destruction cost rate, the exergoeconomic factor, and the relative cost difference. The system's exergy efficiency was 11%, while the electricity cost was between 10.5 EUR/kW and 12.1 EUR/kW, depending on the exergoeconomic approach adopted. Wang et al. [47] performed the multi-objective optimization of an ORC used in geothermal applications. For that purpose, four objective functions were selected: net power output, total product unit cost, greenhouse gas emissions, and ecological life cycle cost. The authors found that R134a showed very attractive thermodynamic and sustainable performances, while R600a had better performances from the economic and environmental aspects when the ORC operated driven by a heat source temperature at 393.15 K.

On the other hand, some studies of ORCs have focused on life cycle analysis. Zhang et al. [48] carried out a study using R134a. The energy yield ratio and the energy sustainability index were 197.52 and 3.97, respectively. The results showed that the sustainability of the ORC system was less than power plants using wind, hydro, and geothermal energies, but considerably higher than plants using fossil fuels. Li [49] performed an investigation of the environmental impact using diverse fluids. Working fluids with low GWP could reduce the emissions to the ambient by between 50% and 84%, compared to fluids with high GWP. The analysis reported that R600 and R123 were the best fluids at low heat source temperatures, while toluene was the best fluid at high temperatures. Yi et al. [50] reported that high condenser and evaporation temperatures and relatively high pinch point temperature differences are beneficial to minimize the environmental impacts.

3.2. Experimental Studies

Pintoro et al. [51] reported the results of an ORC driven by hydrothermal energy at temperatures between 60 °C and 100 °C, using R134a and R245fa as working fluids. A maximum efficiency of 5.62% was obtained with R245fa, achieving a power production of 1909 W. Boydak et al. [52] reported the results of an ORC operating with R134a and driven by low-temperature waste heat obtained from a cement industry in Turkey. The thermal efficiencies varied between 10% and 25%. The turbine produced an average output power of 5.16 kW. Lin et al. [53] reported the experimental assessment of a 10 kW ORC using a scroll expander using R245fa. The authors analyzed the expander pressure ratio and degree of superheating on the system's performance. The highest net thermal and electrical efficiencies were 8.9% and 7.9%, respectively.

Prasetyo et al. [54] analyzed how the degree of superheat in the working fluid affects the performance of an experimental ORC using R123. The authors found that the superheating of the working fluid to higher temperatures favored the power produced; however, the system efficiency decreased, due to the decrease in heat transfer inlets [54], achieving a maximum thermal efficiency of 8.6%, with a power generation of 1.37 kW. A similar study was carried out by Alshammari et al. [55], who analyzed the effect of different working fluids (dry, wet, and isentropic) at different conditions (near the saturated vapor curve or on the superheated area). The system analyzed was an ORC taking advance of waste heat from a 7.5 L heavy-duty diesel engine. The authors found that under the superheated region, the R21 (wet fluid) offered the best cycle performance (12.65%), while near the saturated vapor curve, the maximum cycle performance was obtained with R141b (isentropic fluid). Similar results were obtained for the turbine's isentropic efficiency, since in the superheated region this parameter reached a maximum value of 82% for the wet fluid, while near the saturated vapor curve, isentropic and dry (R123) fluids achieved 80.9% and 80.3%, respectively.

Abbas et al. [56] reported the experimental results of two ORCs operating in cascade, using cyclopentane in the high-temperature cycle and propane, butane, and pentane in the low-temperature cycle, at temperatures between 180 °C and 280 °C. The maximum turbine power, energy, and exergy efficiencies were 4.92 kW, 5.5%, and 20.2%, respectively. Ozdil and Segmen [57] implemented an exergoeconomic analysis of an ORC using R245fa operating in Turkey. The results showed that the exergy cost was 11.05 USD/GJ, with a PBP of 3.27 years. Surindra et al. [58] reported the results of a geothermal ORC installed in Indonesia using R245fa, R123, and mixtures of these. The highest efficiencies were obtained using R123 varying between 9.4% and 13.5%. Özkaraca et al. [59] optimized a binary geothermal power plant installed in Turkey, driving two ORCs using n-pentane, one at 164 °C and the other at 136 °C. The maximum exergy efficiency was 23.92%. Also, it was found that the components with the highest irreversibilities were the condensers, followed by the evaporators. These results were opposite to the results reported by Ali et al. [60] and Li [61], who found that the highest irreversibilities occurred in the evaporator. This behavior is explained by the fact that in the analyzed plant the condenser was cooled by air instead of water, as used by the other authors. Unverdi and Cerci [62] analyzed a similar system installed in Turkey using n-pentane; in this case, the energy and exergy efficiencies were 5.89% and 33.8%, respectively.

Moradi et al. [63] reported the performance of a non-regenerative micro-scale ORC operating with R134 at heat source temperatures varying from 120 °C to 138 °C. For most of the conditions, the expander and pump's isentropic efficiencies were between 35% and 55% and from 17% to 34%, respectively. The maximum net power achieved was 200 W. Peris et al. [64] carried out an experimental study of an ORC utilizing waste heat (120–170 °C) from a ceramic industry. The system was a regenerative ORC operating with R245fa, designed to produce 20 kW of electrical power. Its electrical efficiency varied between 9.8% and 11%. Later, Peris et al. [65] reported the thermoeconomic optimization for this system, focusing on the overall efficiency, which increased from 6.83% to 7.31%. The optimization result showed that the project investment cost diminished from USD 94,576 to USD 81,213, and the specific investment cost from 7667 USD/kW to 6199 USD/kW.

Other studies offer a general approach to ORCs. Landelle et al. [66] presented an analysis of a hundred ORC experimental prototypes. More than thirty working fluids were used, but R245fa, R123, and R134a were the most used. It was reported that 73% of the systems used plate heat exchangers, followed by shell and tube. Most of the developed prototypes produced power between 1 and 10 kW, with electrical efficiencies varying from 1% to 11%. Eyidogan et al. [67] reported electricity power production in Turkey using ORCs operating with low and medium heat-source temperatures. The authors reported that the current installed capacity of ORC was 6.5 MWe, 197 MWe, and 1 MWe using biomass, geothermal, and industrial waste heat, respectively. The PBP for most of the installed plants was 2.7 years, except for the plants using waste heat, whose PBP was reported to be between 5 and 8 years, due to the lack of incentives. As for the heat source, Zhai et al. [68] analyzed the general characteristics of several heat sources, finding that 55.58% of the installed power capacity of ORCs was driven by geothermal energy, followed by biomass (33.01%), waste heat from gas turbines (3.7%), waste heat from industry (3.64%), solar (3.04%) and internal combustion engines (1.03%).

3.3. Discussion of Basic and Experimental ORCs

The modeling of the basic cycles has been carried out at temperatures from 60 °C using fluids such as R600, R32, R290, and R410a [29], and up to 350 °C using propyne, cis-butene, iso-hexane, and cyclohexane [19]. At temperatures lower than 120 °C, fluids such as R123, R134a, R600, R290, R1234yf, and R245fa have been the most efficient. The highest thermal efficiency of 14.6% was obtained using R600, followed by 12.2% using HFE7000, and 12.0% using R245fa. At temperatures between 120 °C and 240 °C, the highest efficiencies were achieved using benzene and methanol, achieving a thermal efficiency of 18.5%, while at temperatures higher than 240 °C, a thermal efficiency as high as 29% was achieved utilizing toluene [11], followed by 21.43% using cyclohexane [19].

From the research focused on the working fluids, it was found that the dry or isentropic fluids are the most suitable for use in microturbines, since higher efficiencies can be achieved, while also avoiding blade damage to the turbine caused by wet vapor [12,13]. Dry fluids with turning points higher than 200 °C are the best for achieving higher efficiencies [11]. It was also found that by utilizing zeotropic mixtures, the efficiencies could be better than those achieved with pure fluids [42].

Regarding thermoeconomic studies, it was found that the PBP of G-ORCs varied considerably, depending on the driven temperature and the drilling costs, since this parameter for an ORC operating at 150 °C is about 4 years, while when it operates at 100 °C this parameter increases up to 8.9 years [38]. The best fluids from the thermoeconomic point of view were R1234yf and cyclohexane.

From the life cycle analysis, it was shown that although the sustainability values of the ORCs were lower than those of power plants using renewable energies, they were considerably higher than those of plants using fossil fuels. From the environmental point of view, R600 and R123 were the best working fluids at low heat source temperatures, while toluene was the best fluid at high temperatures [50].

As for the experimental systems, Table 1 shows the main operating parameters to assess. In this table and the following, the thermal efficiency is determined as indicated by Equation (1):

$$\eta_T = \frac{\dot{W}_{net}}{\sum \dot{Q}_{in}} = \frac{\sum \dot{W}_{out} - \sum \dot{W}_p}{\sum \dot{Q}_{in}} \quad (1)$$

where $\dot{W}_{net}$ is the net power produced by the system, which is calculated as the difference between the power produced by the turbine or turbines (in the case of two-stage or other complex systems) minus the power supplied by the pump or pumps. $\dot{Q}_{in}$ represents the thermal energy supplied to the system through one or more heat exchangers.

Table 1. Operating parameters and main results for the experimental ORCs.

Reference	System Layout	Conditions	Working Fluid	Output	Efficiency (%)		Payback Period
					Thermal	Exergy	
Pintoro et al. [51]	Basic	T_{HS} = 100 °C	R134a and R245fa *	1.9 kW	5.62	-	-
Boydak et al. [52]	Basic	T_{HS} = 205 °C	R134a	5.16 kW	25.0	62	-
Lin et al. [53]	Basic	T_{HS} = 120 °C	R245fa	10 kW	8.9	63.2	-
Prasetyo et al. [54]	Basic	T_{HS} = 120 °C	R123	1.37 kW	8.6	-	-
Abbas et al. [56]	Cascade two ORC	T_{HS} = 280 °C	Cyclopentane, propane, butane, and pentane	4.92 kW	5.5	20.2	-
Ozdil and Segmen [57]	Basic	-	R245fa	-	-	38.79	3.27 years
Surindra et al. [58]	Basic	T_{HS} = 120 °C	R245fa and R123 *	6.5 kW	13.5	-	-
Özkaraca et al. [59]	Recuperative	T_{HS1} = 164 °C T_{HS2} = 136 °C	n-pentane	15 MW	-	23.92	-
Unverdi and Cerci [62]	Basic	T_{HS} = 84.5 °C	R134a, R143a, R152a, R600 *, R290, and R227ea	2.5 MW	12.6	51.2	-
Landelle et al. [66]	Basic	-	R245, R123, and R134a	100 kW	11.0	30	

* Most efficient working fluid.

Analogously, the exergy efficiency reported in the tables is estimated as shown in Equation (2):

$$\eta_{EX} = \frac{\dot{W}_{net}}{\sum \dot{E}x_{in}} = \frac{\sum \dot{W}_{out} - \sum \dot{W}_{p}}{\sum \dot{E}x_{in}} \quad (2)$$

where the term $\dot{E}x_{in}$ is the exergy supplied to the heat exchanger. The exergy of the work is the work itself, so the numerator does not change.

It is important to mention that there are other systems, such as those proposed for producing power and cooling simultaneously, among other outputs, in which the authors define other parameters such as the EUF, which is the addition of the net power plus the cooling load produced by the system; however, those specific parameters are not included in the tables.

As for the experimental systems, the highest thermal efficiency (25%) was obtained using R134a with the heat source at 205 °C [52]. The next efficient system (13.5%) utilized R123 at 120 °C [58]. As was previously stated, most of the installed ORCs have been driven by geothermal sources. For example, in Turkey, the installed capacity of ORCs driven by geothermal energy is 6.5 MWe, followed by 197 MWe produced by biomass, and 1 MWe from industrial waste heat. The PBP for most installed plants operating with renewable energies is less than 3 years.

Although many working fluids have been used in the ORCs, most of the systems have operated with R245fa, R123, and 134a [66]. At the same operating conditions, R123 achieved a higher efficiency than R245fa, showing it to be a better fluid from the thermodynamic point of view, but of course, many other aspects such as environmental impact and safety have to be considered. On the other hand, it was observed that most of the experimental systems produced net outputs between 1 kW and 10 kW, using microturbines as expanders. Also, it is reported that 73% of the systems use plate heat exchangers [66].

4. Recuperative, Regenerative, Reheated, and Supercritical ORCs

Regarding recuperative ORCs, Algieri and Šebo [69] analyzed a system using isobutane, isopentane, and R245ca. The maximum thermal efficiency was 12% for the basic cycle and 14% for the recuperative using R245ca. The thermal efficiencies were always higher with the recuperative ORC than with the basic cycle. Canbolat et al. [70] modeled a recuperative cycle using dry fluids. The highest energy and exergy efficiencies were 16.7% and 60%, respectively, using R245fa. Zhang et al. [71] analyzed the performance

of the same system, but using R245fa, R1234ze(Z), R601a, and R600a. The highest exergy efficiencies were obtained using R600a, reaching values around 34%. Proctor et al. [72] modeled a recuperative ORC using n-pentane. The model was validated against the plant data, obtaining a maximum power output deviation of 0.24%. Uusitalo et al. [73] analyzed the performance of the same system operating with diverse hydrocarbons, siloxanes, and fluorocarbon fluids. The efficiencies were higher at higher fluid critical temperatures if the evaporation pressure was slightly lower than the critical pressure. Ali et al. [60] modeled the same system, using thirty-three working fluids. At a heat source temperature of 90 °C, the highest thermal efficiencies were obtained with RC318 and R227ea, with values around 6.5%. At temperatures of 170 °C, the highest efficiencies were obtained with R123, R236ea, and R114, with values of 19.5%, 15.6%, and 15.3%, respectively. From the exergy analysis, it was determined that more than 50% of the exergy destroyed in the system occurred in the evaporator. These results are in concordance with those published by other authors [19,31,45].

Pezzuolo et al. [74] developed a tool for fluid selection. Eighty fluids were analyzed at 170 °C. The maximum thermal efficiencies of around 25.6%. were obtained with benzene, toluene, and cyclopentane. Agromayor and Nord [75] modeled the same cycle. Eighty fluids were first analyzed, but after considering safety and environmental aspects, twenty-nine were selected at temperatures between 100 °C and 250 °C. The exergy efficiency strongly depends on the choice of the working fluids for a basic ORC, but not for the recuperative cycle. The efficiencies of the recuperative ORC were, in general, higher than those obtained with the basic ORC, which is in concordance with the results published by Algieri and Šebo [69]. Regarding thermoeconomic studies, Huster et al. [76] analyzed a recuperative ORC using isobutane. The LCOE varied between 0.04 USD/KWh and 0.06 USD/kWh. Preißinger and Brüggemann [77] compared the performance of a recuperative cycle using alkylbenzenes, alkanes, and siloxanes, and found that the best working fluid was hexamethyl-disiloxane, with a PBP lower than 5 years. Heberle et al. [78,79] carried out a similar study, but for a system driven with solar and geothermal energy, over a whole year in Turkey. The lowest electricity cost was 0.145 USD/kWh, while Ahmadi et al. [7] reported that, for their analysis, the cost was 0.3 USD/kWh. On the other hand, Stoppato and Benato A. [80] reported the life cycle analysis of a recuperative ORC driven by biomass using R123, R245fa, and R1233zd. According to the authors, the use of R1233zd guarantees the same system performance as using the other fluids, but with a considerably lower impact on the environment. Lu et al. [81] analyzed the performance of a basic and a recuperative ORC using the zeotropic mixtures. The highest power and thermal efficiencies were 36.36 kW and 11.11%, respectively, using R245fa/R600a. It was observed that the thermal efficiencies were higher with the recuperative than with the basic ORC, as it was reported by Algieri and Šebo, J. [69] and Agromayor and Nord [75]. Tiwari et al. [82] modeled the same ORC using the zeotropic mixture R600/R601 driven by solar energy. The results showed that the thermal and exergy efficiencies were 12.3% and 58.2%, respectively. Van Erdeweghe et al. [83] addressed a thermoeconomic study of a G-ORC, and found that it was not economically feasible for the system to be installed in Belgium; however, the system would have a more favorable economic situation in a country with higher brine temperatures or higher cost of electricity, e.g., higher than 79.5 USD/MWh.

4.1. Comparison between Recuperative, Regenerative, and Reheated ORCs

Imran et al. [84] analyzed the theoretical performance of a regenerative G-ORC and compared the results with a basic ORC and a recuperative ORC using R600, R600a, R601, R601a, R245fa, and SES36. The best fluid was R245fa for all the configurations. The energy and exergy efficiencies were the highest with the recuperative and regenerative cycles, but the specific costs were also the highest. Using the R245fa, the maximum exergy efficiency and the minimum cost for the regenerative cycle were 55.93% and 0.2567 USD/MWh, respectively. Similar results were also found by other authors [61,85,86]. From the exergy analysis, it was found that the exergy destruction was lower in the recuperative and

regenerative cycles compared to the basic and reheated ORCs [61,86]. Yang and Yeh [87] reported the results of the thermoeconomic optimization of a reheated G-ORC. The authors analyzed six working fluids with low global warming potential. It was found that the minimum costs were obtained with R600, followed by R600a.

More recently, Nondy and Gogoi [10] compared different configurations, including basic, recuperative, regenerative, and recuperative–regenerative ORC (Figures 1–3 and 5) from the exergoeconomic point of view. Their analysis considered a multi-objective optimization for improving the performance of each configuration, using the exergy efficiency and the system cost as the objective functions. The authors found that under optimal conditions, the recuperative–regenerative configuration showed the best performance, followed by the regenerative, and the recuperative systems. Zhar et al. [88] also analyzed and compared three ORC configurations: the basic, reheated, and regenerative cycles, operating with four different working fluids, from the energy, exergy, and economic perspectives. In this case, the regenerative cycle showed the best energy efficiency, regardless of the working fluid.

Javed and Tiwari [89] also compared the basic, recuperative, and regenerative cycles from the energy and economic perspectives, using toluene, nonane, decane, and dodecane. This study proved that, under ideal operative conditions, the regenerative cycle operating with toluene showed the best performance, obtaining a maximum first-law efficiency of 37.01%.

4.2. Supercritical ORC

A cycle is supercritical if the maximum pressure is higher than the critical pressure, as shown in Figure 8.

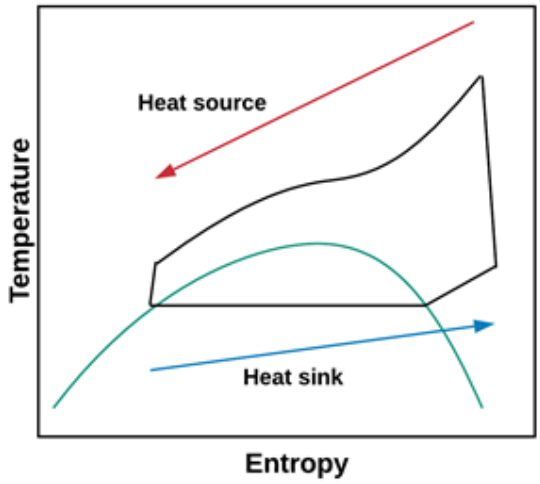

Figure 8. T-s diagram of a supercritical ORC.

Liu et al. [90] analyzed the performance of a supercritical G-ORC using diverse fluids with critical temperatures ranging from 66.0 °C to 113.3 °C. The highest efficiency (11.18%) was obtained with R152a, which had the highest critical temperature. The authors also analyzed a subcritical ORC using zeotropic mixtures, and found that the thermal efficiencies were around 3.8% higher using zeotropic mixtures, as was reported by Oyewunmi and Markides [42]. Manente et al. [91] analyzed the same cycle, and compared the results with a subcritical ORC. The results showed that, on average, the supercritical ORC produced up to 20% more power than the subcritical ORC. The highest exergy efficiency values, around 46%, were obtained with supercritical cycles using R1234yf, R134a, and R1234ze(E). Chagnon-Lessard et al. [92] optimized a supercritical G-ORC using 36 working fluids. The results were summarized in charts, together with a correlation that may be used as an efficient tool for designing optimal geothermal power plants. Moloney et al. [93] analyzed a supercritical G-ORC with a recuperator using twenty fluids. The best first- and second-law performances were 16.2% and 52.3%, using R1233zd(E).

Erdogan and Colpan [94] compared the performance of a supercritical ORC with a recuperator with a subcritical ORC. It was found that 44.12% more power was produced with the supercritical than with the subcritical ORC. Lukawski et al. [95] performed a similar study using thirteen different fluids, and found that the supercritical cycles achieved thermal and exergy efficiencies of up to 17% more, compared to the higher than those for subcritical ORCs. Song et al. [96] analyzed the same cycle using fifty-two different fluids at four typical temperatures. It was found that at a specific heat source temperature, the energy efficiency increases with the increment of the critical fluid temperature and decreases with increasing fluid dryness. Wang et al. [97] theoretically compared the performance of a basic and a supercritical G-ORC operating with thirty fluids, with the best being R134a, R32, R600a, and R22. From the comparison with subcritical ORCs, for all the working fluids, on average, the energy efficiencies were around 14.5%, while for supercritical ORCs, the efficiencies were around 17.2%. Cakici et al. [98] analyzed the same system driven with geothermal and solar energy, using R134a, R124, R142b, R227ea, and isobutane. The maximum energy and exergy efficiencies were 12% and 45%, respectively, using R134a.

4.3. Discussion on Recuperative, Regenerative, Reheated, and Supercritical Cycles

Table 2 shows the most relevant data for the recuperative, regenerative, reheated, and supercritical ORCs. The studies analyzing the working fluids found that the fluorocarbons and hydrocarbons with low critical temperatures were the best for low heat source temperatures, while the siloxanes and the hydrocarbons with high critical temperatures were the most suitable at high temperatures [73]. Diverse authors coincide with the fact that the R245fa is the most efficient fluid when compared with some hydrocarbons and other working fluids at temperatures lower than 140 °C [69,84,85], but at temperatures around 170 °C, the best working fluids are ethanol, benzene, and toluene, with values of 24.2%, 23.2%, and 22.9%, respectively [74].

Table 2. Operating parameters and main results for the different configurations of ORCs.

Reference	Most Efficient Cycle	Conditions	Working Fluid	Output	Efficiency (%)		Component with the Highest Irreversibilities	LCOE
					Thermal	Exergy		
Algieri and Šebo [69]	Recuperative	T_{HS} = 139 °C	Isobutane, isopentane and R245ca *	4.0 kW	14.0	-	-	-
Canbolat et al. [70]	Recuperative	T_{HS} = 127 °C	R142b, R227ea, R245fa *, R600 and R600a	-	16.7	60.0	Evaporator	-
Zhang et al. [71]	Superheated recuperative	T_{HS} = 100 °C	R245fa, R1234ze(Z), isopentane e isobutane *	24.0 kW	26.38	34.0	-	-
Uusitalo et al. [73]	Recuperative	T_{HS} = 300 °C	Hydrocarbons, siloxanes and fluorocarbons	31.1 kW	25.2	-	-	-
Ali et al. [60]	Basic, Recuperative	T_{HS} = 165 °C	Butane, Isobutane, Isopentane *, etc.	89.61 kW	19.83	-	Evaporator	-
Pezzuolo et al. [74]	Basic, Recuperative	T_{HS} = 170 °C	Benzene *, toluene, cyclopentane, etc.	4.0 MW	25.7	37.60	-	0.118 USD/kWh
Agromayor and Nord [75]	Simple, Recuperative	T_{HS} = 600 °C	Alkylbenzenes, alkanes and siloxanes	550 kW	-	30.0	-	-
Lu et al. [81]	Basic, Recuperative	T_{HS} = 140 °C	Zeotropic mixtures R601a/R600 and R245fa/R600a	36.4 kW	11.11	-	-	-
Imran et al. [84]	Basic, Recuperative, Regenerative	T_{HS} = 160 °C	R600, R600a, R601, R601a, R245fa * and SES36.	68.4 kW	14.02	55.93	-	-
Wang et al. [85]	Basic, Recuperative, Regenerative	T_{HS} = 150 °C	Fourteen working fluids, R245fa *	-	12.0	48.0	-	-
Li [87] and Li [61]	Basic, Regenerative, Recuperative, Reheated	T_{HS} = 130 °C	Fourteen working fluids, R245fa *	-	13.2–13.8	-		0.26 USD/kWh

Table 2. *Cont.*

Reference	Most Efficient Cycle	Conditions	Working Fluid	Output	Efficiency (%)		Component with the Highest Irreversibilities	LCOE
					Thermal	Exergy		
Yang and Yeh [87]	Reheated	T_{HS} = 94 °C	R600 *, R600a, R1233zd, R1234yf, R1234ze.	332.7 kW	8.29	-	-	0.3 USD/kWh
Liu et al. [90]	Basic Supercritical	T_{HS} = 130 °C	R125, R218, R143a, R32, R290, R134a, R227ea, R1234ze(E), and R152a *	599.1 kW	11.18	-	-	-
Manente et al. [91]	Supercritical	T_{HS} = 150 °C	R1234yf *, R134a, R1234ze (E), R1234ze (Z), R245fa, R600a	900.8 kW	10.64	-	-	-
Moloney et al. [93]	Binary, Single flash	T_{HS} = 240 °C	Twenty different working fluids	150 kW	19.0	50.0	Turbine	-
Lukawski et al. [95]	Basic, Recuperative supercritical	T_{HS} = 220 °C	Thirteen working fluids, R134a *	120 kW	19.0	-	-	-
Cakici et al. [98]	Recuperative supercritical	T_{HS} = 160 °C	R134a *, R124, R142b, R227ea, and isobutane	5800 kW	12.0	45.0	Parabolic trough solar collectors	-

* Most efficient working fluid.

From the comparison of the different configurations of ORCs operating in subcritical mode, it was found that the efficiencies of recuperative ORCs were up to 15% higher than those of a basic ORC [69,75]. Using R245fa as working fluid and at an evaporation temperature of 130 °C, the most efficient cycles were the recuperative and the regenerative ORCs, achieving efficiencies of around 13.2%, while for the basic and reheated ORCs the efficiencies were around 12% [61,84,86]. Regarding supercritical ORCs, it was found that at temperatures lower than 150 °C these cycles produced up to 20% more power than subcritical ORCs, achieving maximum power outputs of around 44.12% [91,94]. The highest exergy efficiency values, around 46%, were obtained with supercritical using R1234yf, R134a, and R1234ze(E). At temperatures between 170 °C and 240 °C, it was reported that the highest efficiencies were obtained with R1233zd(E), butane, isopentane, pentane, and neopentane [93]. It was found that the critical temperature and fluid dryness considerably affected the system performance. Considering not only the thermodynamic efficiencies, but also the toxicity, flammability, and environmental friendliness, the best working fluids were R134a, R600, R601, and R123, in the range of 100 to 300 °C [96]. From the exergy analysis, it was found that the maximum irreversibilities (contributing more than 50%) occurred in the evaporator, followed by the condenser, expander, and pump [60,61,86]. Finally, from the thermoeconomic studies, it was estimated that the lowest LCOE was obtained with the reheated ORC, followed by the recuperative, the basic, and the regenerative ORCs, with values of 0.26 USD/kWh, 0.28 USD/kWh, 0.29 USD/kWh, and 0.3 USD/kWh, respectively [61,86].

5. Two-Stage ORC

Currently, there is a great variety of two-stage ORC configurations (sometimes called double-pressure ORCs), but all of them have in common the fact that the heat is supplied to the working fluid at two pressure levels, to increase power production and/or system efficiency.

Sun et al. [99,100] compared the performance of a two-stage ORC as shown in Figure 9, using R21, R114, and R245fa. This configuration is also known as a conventional two-stage ORC. Using R245fa, the highest power and exergy efficiencies were 818.6 kW and 5.85%. These values were higher than those obtained with the basic ORC, reaching values of 735.1 kW and 5.28%, respectively. Manente et al. [101] modeled a similar system, but the working fluid leaving the low-pressure turbine (LPT) was reheated again. The analyzed fluids were R134a, isobutane, isopentane, and cyclopentane. When the critical temperature was close to the heat source inlet temperature, the efficiencies of the proposed cycle were up to 29% higher than those of a basic ORC. At 150 °C, the thermal efficiencies varied between 10.3% and 11.1% for all the fluids, while at 200 °C the efficiencies varied between 14% and

15.5%. Wang et al. [102] performed a thermoeconomic evaluation of the same configuration, but using R1233zd as a working fluid. The electricity production costs ranged from 0.041 to 0.056 USD/kWh at evaporator temperatures from 140 °C to 180 °C.

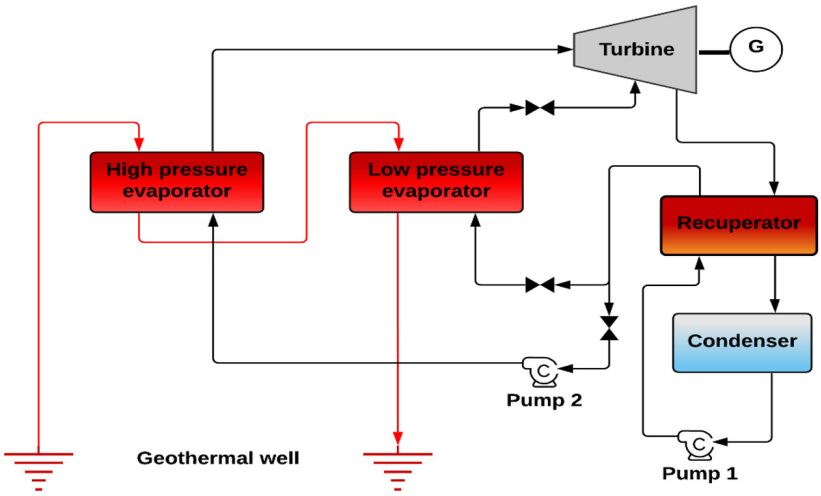

Figure 9. Thermodynamic two-evaporator ORC using a recuperator proposed by Sun et al. [99]. Different colors in Figure represent different temperature levels.

Fontalvo et al. [103] compared the performance of a two-stage ORC with a basic and a regenerative ORC, operating with 2,3,3,3-Tetrafluoropropene (R1234yf), (trans-1,3,3,3-Tetrafluoropropene) R1234ze(E), and (cis-1,3,3,3-tetrafluoroprop-1-ene) R1234ze(Z). Unlike the cycle proposed by Sun et al. [99], the proposed cycle had two pumps at the exit of the condenser. One pumped the working fluid to the LPE, while the other pumped the fluid to the HPE. The highest energy efficiency was 18%, using R1234ze(E). It was concluded that the proposed cycle increased the power by 20%, compared to the basic ORC. The minimum electricity production cost was 0.3 USD/kWh, with a PBP of 8 years. Similar values were also found by Ahmadi et al. [7]. Braimakis and Karellas [104] performed the optimization of three different configurations of ORCs with and without regeneration, as shown in Figure 10. For the non-regenerative cycles, the thermal efficiencies were 20.9%, 20.53%, 19.94%, and 18.02%, for the CF-ORC, O-ORC, CB-ORC, and ORC, respectively. The efficiencies for the three proposed configurations increased by around 15% when regeneration was included. These results showed that regeneration is essential in ORCs, and its effect could be even more important that the development of more sophisticated ORCs. The same authors [105] modeled a two-stage ORC integrating two single ORCs with several fluids. That system achieved exergy efficiencies up to 25% higher than those of basic ORCs. At temperatures lower than 150 °C, the exergy efficiencies varied between 20% and 30%, and were very similar for all the fluids; however, at temperatures close to 300 °C, the best second-law efficiencies were around 50%, obtained with cyclopentane, cyclohexane, and toluene. Liu et al. [106] performed an exergy analysis of the same cycle using R600, R600a, R601a, and R245fa as working fluids. The highest exergy efficiency of 41% was obtained using R600a, which was 9.4% higher when compared with a single-stage cycle.

Li et al. [107,108] and Wang et al. [109] modeled a two-stage ORC driven by geothermal energy operating with R245fa. The system was modeled at temperatures between 65 °C and 100 °C. The best energy and exergy efficiencies were 9.2% and 42%, respectively, obtained with a heat source at 100 °C. Li et al. [110] optimized a two-stage ORC using two evaporators and a preheater using nine working fluids. The highest efficiencies were 6.1% at 100 °C and 13.2% at 200 °C, using R245fa. Wang et al. [111] analyzed the same cycle, but operating with isobutane. It was estimated that there was an electricity production cost of 0.24 USD/kWh at 100 °C and 0.14 USD/kWh at 160 °C.

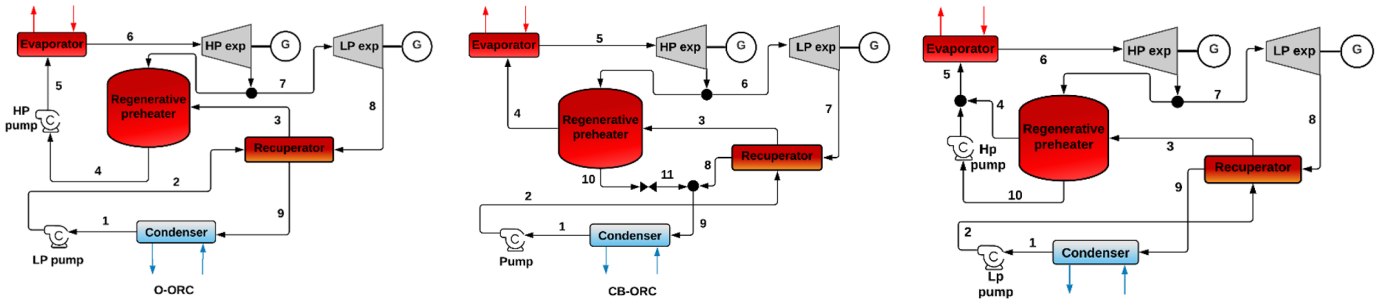

Figure 10. Double-stage regenerative ORC configurations with (**a**) Open preheater; (**b**) Closed preheater with backward bleed condensate circulation; (**c**) Closed preheater with forward bleed condensate circulation [104]. Different colors in Figure represent different temperature levels.

Kazemi and Samadi [112], and Samadi and Kazemi [113] proposed an ORC as shown in Figure 11, using isobutane, R123, and isobutane/isopentane. The maximum energy and exergy efficiencies were obtained using R123, achieving values of 15.31% and 54.25%, respectively. The minimum electricity production cost was 3500 USD/kW.

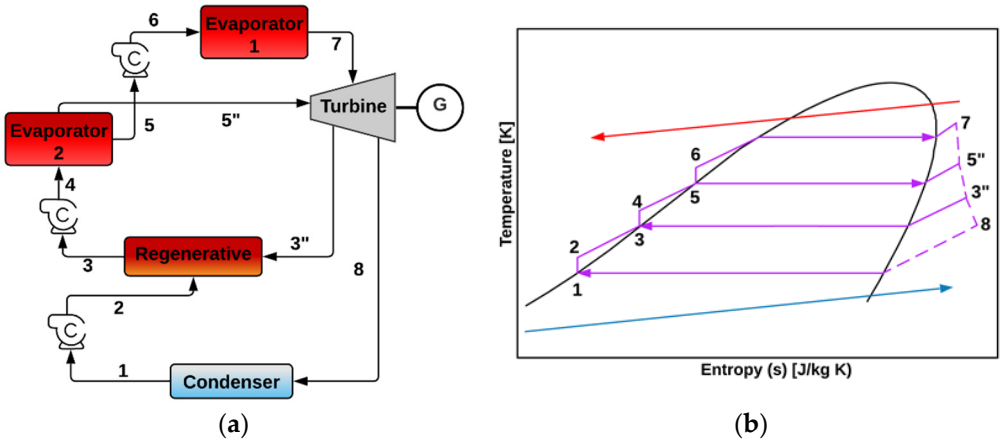

Figure 11. Double-stage ORC [112]. (**a**) Schematic diagram; (**b**) T-s diagram. Figure modified from Kazemi and Samadi [112]. Different colors in Figure represent different temperature levels; different numbers mean different thermodynamic states for the cycle.

Nami et al. [114] carried out an exergy analysis of the same cycle proposed by Kazemi and Samadi [112], showing that the low-pressure evaporator, high-pressure evaporator, and condenser were the components with the highest exergy destruction, contributing 38.11%, 29.98%, and 15.93%, respectively. Luo et al. [115] analyzed the performance of a two-stage ORC using a condenser with liquid separation operating with the zeotropic mixture R245fa/R365mfc. Although the system had only two evaporators, due to the change in the boiling point of the zeotropic mixture, the system could operate at multiple pressures, closely matching the temperature of the heat source. The net power produced was between 13.05% and 26.18% higher than that of a basic ORC using the same zeotropic mixture. The use of the condenser with liquid separation leads to an increase of up to 8.22%, compared to a traditional ORC. Zhou et al. [116] analyzed a two-stage ORC where the vapor at the exit of the high-temperature ORC mixed with the vapor of the low-temperature evaporator before entering the low-pressure turbine. The maximum energy and exergy efficiencies were 18.33% and 62.37%, respectively. Surendran and Seshadri [117] proposed a transcritical regenerative two-stage ORC, as shown in Figure 12, using cyclopentane driven by waste heat at two different temperature levels. The power outputs were 23% and 16% higher when compared with a basic and a conventional two-stage ORC, respectively.

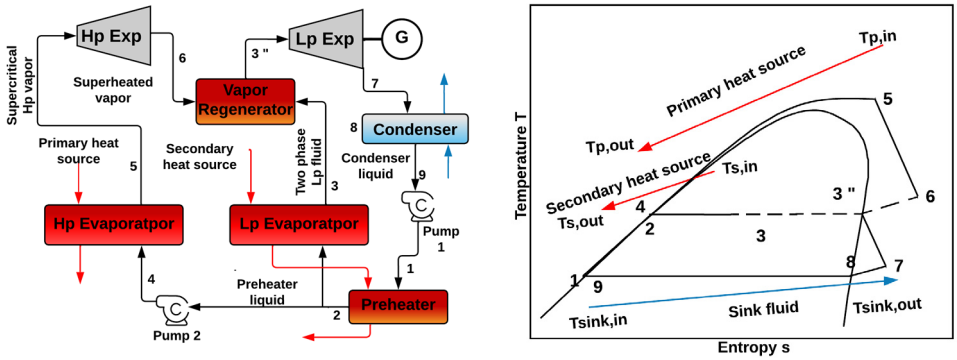

Figure 12. Double-stage ORC [117]. (**a**) Schematic diagram; (**b**) T-s diagram. Figure modified from [117]. Different colors in Figure represent different temperature levels.

Li et al. [118] modeled an ORC with two evaporators, a high-pressure turbine and a low-pressure turbine. The results showed that, in general, the ORC driven by the dual-level heat sources improved the system performance compared with a single-level heat source. Heberle et al. [119] performed a life cycle assessment of a two-stage ORC. In the analysis, the authors considered the substitution of R245fa and R134a by working fluids with low environmental impacts such as R1233zd and R1234yf. It was found that the exergy efficiency decreases by 2%, but the global warming impact reduces by 78% when using R123zd instead of R245fa. Sadeghi et al. [120] compared the performance of three different configurations of ORC powered by geothermal energy operating with ten zeotropic mixtures. The analyzed configurations were a basic ORC, a parallel two-stage ORC, and a series two-stage ORC, as shown in Figure 13. Using zeotropic mixtures instead of a pure fluid, such as R245fa, leads to an efficiency increase of about 25% in the three ORC configurations. Additionally, it was reported that the series two-stage ORC was the most efficient configuration. The highest energy and exergy efficiencies achieved by the series two-stage ORC were 9.79% and 57.5%, respectively.

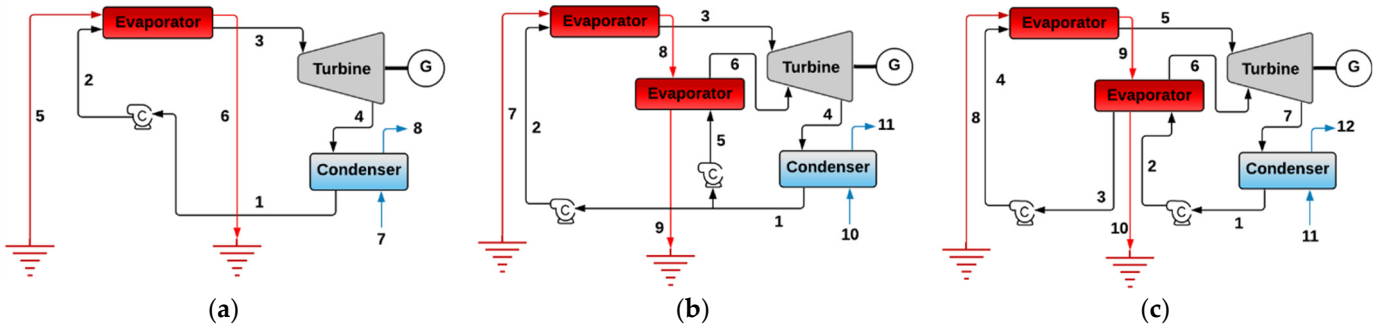

Figure 13. Configurations analyzed by Sadeghi et al. [120] (**a**) Simple ORC; (**b**) Parallel two-stage ORC; (**c**) Series two-stage ORC. Different colors in Figure represent different temperature levels for thermal components.

Chagnon-Lessard et al. [121] compared the theoretical performance of four different ORC configurations: a subcritical ORC, a transcritical ORC, a subcritical two-stage ORC, and a transcritical two-stage ORC, using twenty different fluids. In general, the highest efficiencies were obtained using the transcritical two-stage ORC. Wang et al. [122] compared the performance of a two-stage in-series ORC with a dual-level heat source with a similar system but operating with only one heat source. The results showed that the electricity production cost and PBP were always lower with the two-stage ORC with a dual-level heat source. The minimum values were 0.084 USD/kWh and 1.71 years, respectively. Recently, Wang et al. [123] analyzed the exergy performance and fluid selection of a dual-loop ORC,

shown in Figure 14, driven by flue gas at 300 °C. The authors conducted a multi-objective optimization with exergy efficiency, payback period, and annual CO_2 emissions reduction as the objective functions. It was found that using a zeotropic mixture instead of a pure fluid as the working fluid can benefit the system's performance; however, the optimal mass fraction in the mixture depends on each performance parameter and is different for every loop in the ORC. Moreover, the authors found that the use of optimal mixtures significantly affects the exergy efficiency and annual emissions reduction, but does not have an important effect on the PBP.

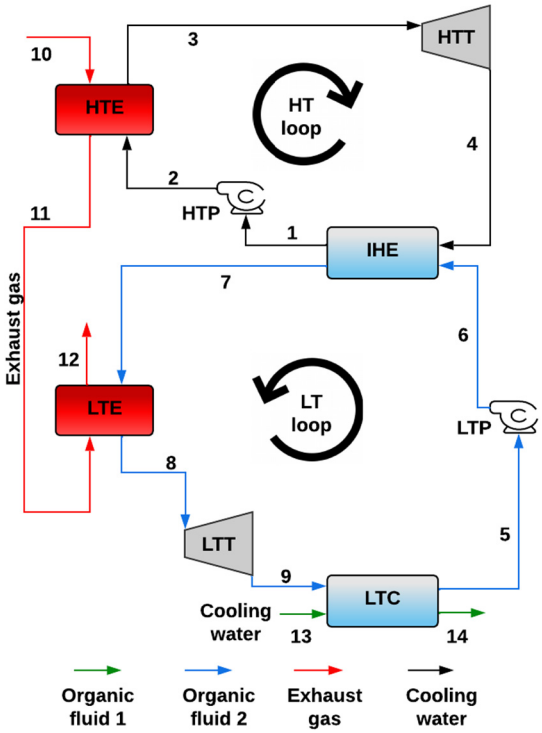

Figure 14. Schematic diagram of the two-stage ORC proposed by Wang et al. [123]. Different colors in Figure represent different temperature levels for thermal components.

Discussion of Two-Stage ORC

There are a considerable number of studies regarding two-stage ORCs proposing diverse configurations; some of them, in addition to the evaporator and condenser, include components such as a recuperator and a regenerator. The use of a regenerator proved to be very convenient, since it increased the thermal efficiencies of the analyzed configurations by up to 15% [104]. A great variety of working fluids have been proposed for the different configurations, but those with the highest efficiencies were R245fa, R123, R1234ze(E) cyclopentane, and isopentane.

From Table 3, it can be seen that the highest thermal efficiencies (about 18%) were obtained by Zhou et al. [116] and Fontalvo et al. [103] with a two-stage regenerative ORC operating at temperatures around 200 °C. At temperatures lower than 150 °C, the highest thermal efficiency (15.31%) was achieved with the system proposed by Kazemi and Samadi [112]. Some of the proposed two-stage ORCs could increase the efficiency between 10% and 20% [99,100,104–106] and the power between 13% and 26% [100,112], compared to the basic cycle configuration. Regarding the cost analysis, the lowest LCOE (0.084 USD/kWh) and a PBP of 1.71 years were reported by Wang et al. [122] for the system consisting of a two-stage series ORC operating with a dual-level heat supply.

Table 3. Operating parameters and main results for the two-stage ORCs.

Reference	Most Efficient Cycle	Conditions	Working Fluid	Output	Efficiency (%)		Cost (LCOE or PBP)	Component with the Highest Irreversibilities
					Thermal	Exergy		
Sun et al. [99,100]	Basic, two-stage *	T_{HS} = 113 °C	R21, R114, and R245fa *	818.6 kW	-	5.85	-	HPE
Manente et al. [101]	Basic, two-stage *	T_{HS} = 200 °C	R134a, R1234ze (Z), isobutane, isopentane, and cyclopentane.	8573 kW	15.36	-	-	-
Wang et al. [102]	Two-stage	T_{HS} = 113.8 °C	R1234zd	614.27 kW	-	-	PBP = 3.99	-
Fontalvo et al. [103]	Two-stage, basic, regenerative *	T_{HS} = 200 °C	R1234yf, R1234ze(E) *, and R1234ze(Z).	33 kW	18.1	60.0	0.3 USD/kWh PBP = 8 years	-
Braimakis and Karellas [104,105]	Basic, two basic operating in cascade	T_{HS} = 100 °C	Butane, pentane, cyclopentane *, cyclohexane, toluene, R134ze, and R134yf.	-	5.0	25.0	-	-
Liu et al. [106]	Basic, two basic operating in cascade	T_{HS} = 140 °C	R600, R600a, R601a, and R245fa	-	-	41.0	-	-
Li et al. [107,108]	Two-stage	T_{HS} = 100 °C	R245fa	9.0 kW	9.2	42.0	-	HPE
Li et al. [110]	Basic, two-stage	T_{HS} = 200 °C	R227ea, R236ea, R245fa *, R600, R600a, R601, R601a, R1234yf and R1234ze(E)	100 kW	13.5	-	-	-
Wang et al. [111]	Basic, two-stage *	T_{HS} = 160 °C	Isobutane	241.7 kW	11.29	-	0.14 USD/kWh	-
Kazemi and Samadi [112]	Three pressure levels	T_{HS} = 134.3 °C	Isobutane and R123 *	-	15.31	54.25	-	Condenser
Samadi and Kazemi [113]	Three different pressure levels	T_{HS} = 124.5 °C	Isobutane, isopentane *	-	13.78	53.02	-	-
Luo et al. [115]	Basic, two basic operating in parallel *	T_{HS} = 195 °C	Isobutane-isopentane (0.9–0.1)	407.62 kW	-	31.77		HPE
Zhou et al. [116]	Two-stage	T_{HS} = 188 °C	Six working mixtures, pentane/Cis-2-butane (0.539/0.461) *	5983.19 kW	18.43	62.96	-	HPE
Surendran and Seshadri [117]	Transcritical regenerative two-stage	T_{HS} = 302 °C	Cyclopentane	349 kW	15.3	17.4	-	HPE
Sadeghi et al. [120]	Basic, two-stage parallel, series, two-stage *	T_{HS} = 100 °C	R407A	940.3 kW	8.53	55.63	-	HPE
Wang et al. [122]	Two-stage series with dual-level HS	T_{HS} = 104 °C	R123	78 kW	6.0	28.0	0.084 USD/kWh PBP = 1.71 years	-

* Most efficient working fluid.

6. Hybrid ORC

Hybrid ORCs are considered to be those systems integrating at least two different technologies to produce one or more different outputs.

Najjar and Qatramez [124] modeled a hybrid system consisting of a single flash geothermal cycle operating a steam turbine and an ORC using n-butane, isobutane, R11, and R123. The highest energy efficiency of 18.76% and net power output of 24,887 MW were obtained with R11. Matuszewska and Olczak [125] proposed a hybrid cycle integrating an ORC, using R245fa, R1233zd(E), and R600, and a Brayton cycle operating at about 550 °C. The heat delivered by the Brayton cycle gas turbine was used to preheat the brine coming from a geothermal well. The highest thermal efficiencies were achieved using R1233zd(E), reaching values up to 19.20% higher in comparison with a basic ORC. Yağlı et al. [126] proposed the adaptation of an ORC to improve the performance of a gas turbine located in a wood production facility. The study analyzed eight different working fluids. The parametric optimization of the cycle required increasing the turbine inlet pressure from 10

to 35 bar. Benzene was the best working fluid in the pressure range of 10 to 25 bar (at the inlet of the turbine), while R123 showed the highest performance for pressures between 25 and 35 bar. For this fluid, the highest values were 1076.76 kW, 21.1%, and 47% for power production and thermal and exergy efficiencies, respectively.

Mokarram and Mosaffa [127] proposed a cycle integrating a steam turbine and a transcritical G-ORC, using R245fa. The system produced 7.2% more power compared to a similar cycle operating in subcritical conditions. The maximum energy and exergy efficiencies were 14.66% and 55.15%, respectively, with a LCOE of 0.2018 USD/kWh. Li et al. [128] proposed a cooling, heating, and power G-ORC as shown in Figure 15, using twenty zeotropic mixtures. At 90 °C, the highest power, cooling capacity, and exergy efficiencies were 92 kW, 2450 kW, and 0.62%, respectively, using R141b/R134a.

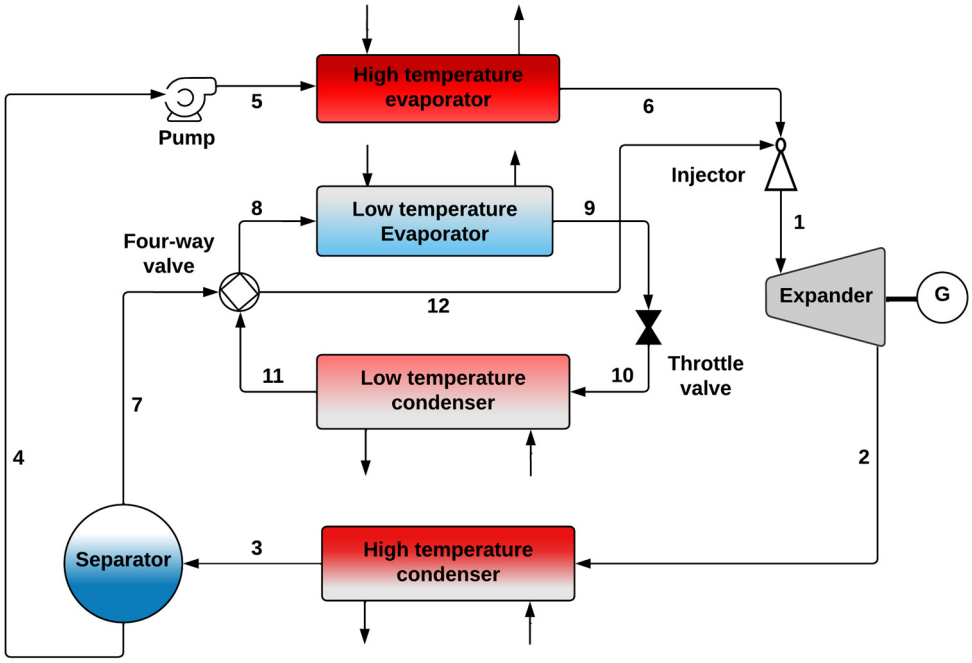

Figure 15. Schematic diagram of the hybrid system proposed by Li et al. [129]. The different colors in Figure represent the different temperature levels in the cycle for thermal components.

Sun et al. [129] modeled a two-stage ORC supplying the residual heat to an absorption cooling system (ACS) for the simultaneous production of power and cooling. Compared to a two-stage ORC, the system enhances the net power produced by 10%. Ehyaei et al. [130] proposed a similar system with R134a. The use of the ACS improved the efficiency from 9.3% to 47.3%, having a minimum electricity cost of 3.3 USD/MWh. Leveni and Cozzolino [131] modeled the same system producing a net power of 5 kW, achieving an exergy efficiency of 40.98%. Wang et al. [132] proposed a similar system, but in this case with an eject-compressor cooling system (ECS). The best energy and exergy efficiencies were 18.1% and 59.1%, respectively, at a geothermal heat source temperature of 190 °C. Jafary et al. [133] also studied the integration of a trigeneration system for the production of combined cooling, heating, and power (CCHP), utilizing a double-effect absorption cooling system as the bottoming cycle of an ORC driven by a solar power plant with parabolic trough collectors (PTC). The authors analyzed two configurations for the power system: the first one considered an internal heat exchanger, while the second one was a regenerative system. The analysis reported a better performance from the energy and exergy perspective for the first configuration.

Jiménez-García et al. [134], also investigated the simultaneous production of power and cooling by the coupling of an ORC and a double-effect absorption cooling system, from the perspective of the first law of thermodynamics. The authors analyzed the system performance using four working fluids for the organic cycle (benzene, toluene, cyclohexane, and methanol) and the NH_3-$LiNO_3$ mixture for the absorption cycle. They found that, for

a wide range of operating conditions, the cooling load was much higher than the power production. Under the operating conditions analyzed (heat source temperature from 160 to 220 °C), the best system performance was obtained with benzene, achieving an energy utilization factor (EUF) of 0.854 and a maximum exergy efficiency of 39.8%.

Lizarte et al. [135] modeled an ORC and a cascade compressor cooling system (CCS) to produce cooling at temperatures between −55 °C and −30 °C. The power produced by the ORC was the input to the cooling cycle. The best COP and exergy efficiencies were 0.79 and 31.6%, respectively. A similar study was published by Li et al. [136], but instead of producing cooling, the system was proposed for power and space heating. The system was modeled for a period of up to 20 years. The annual average COP was 3.8. Marty et al. [137] presented the optimization of a G-ORC using R245fa for the simultaneous production of power and district heating. The geothermal fluid was split into two lines, one used for the ORC and the other used for the district heating network.

Maali and Khir [138] analyzed the optimal operation of an ORC operating with solar and geothermal heat sources, from the energy and exergy perspectives. The analysis was performed considering the conditions of two typical days (summer and winter) in Tunisia. The main sources of irreversibilities were the steam generator, the air-cooled condenser, and the turbine. The power plant performance was optimized by applying a linear regression analysis to relate the volume flow rate and temperature of the heating fluid with solar radiation. The authors found that in winter, an increment from 55 to 75 °C in the geothermal water temperature can improve the plant's exergy efficiency by about 4.35%. However, in summer this parameter did not significantly affect the system performance.

Boukelia et al. [139] also analyzed the integration of solar and geothermal heat sources for electricity production, but considering two production levels: one of them was composed of a parabolic trough solar power plant and a Rankine cycle, while the other was a geothermal power plant using an organic Rankine cycle. For that purpose, the authors performed the design and thermo-economic analyses including nine organic fluids, finding that this configuration raised the power generation by 19.36% with respect to the stand-alone solar plant. They also found that wet fluids were more convenient than dry ones. Thus, the best fluids in this configuration were ammonia, R32, R290, and R143a. Javanshir et al. [140] proposed a system integrating an ORC and a CCS, as shown in Figure 16. The system operated with R134a, R22, and R142a. The best energy and exergy efficiencies were obtained using R143a, and reached 27.2% and 57.9%, respectively. The electricity production cost was 60.7 USD/GJ.

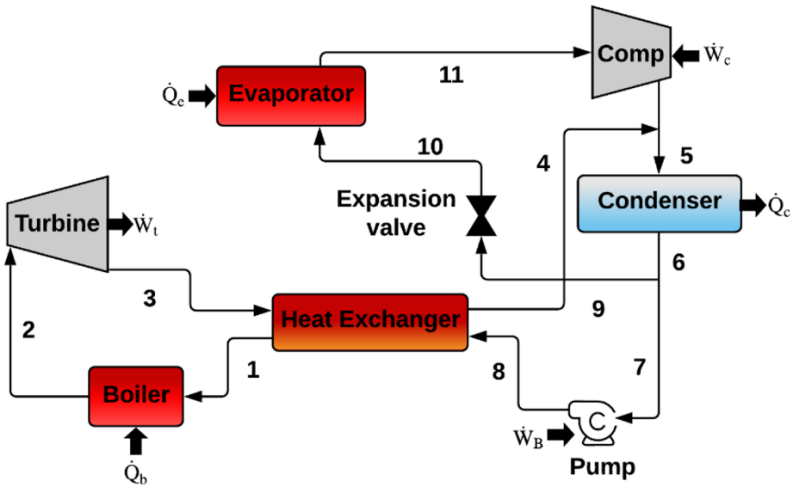

Figure 16. Schematic diagram of the hybrid system proposed by Javanshir et al. [141]. The different colors in Figure represent the different temperature levels in the cycle for thermal components.

Pashapour et al. [141] proposed a system integrating a Brayton cycle, an ORC, and an ACS for the production of power, heating, and cooling, as shown in Figure 17. The highest exergy efficiency and COP were 50.6% and 0.5, respectively.

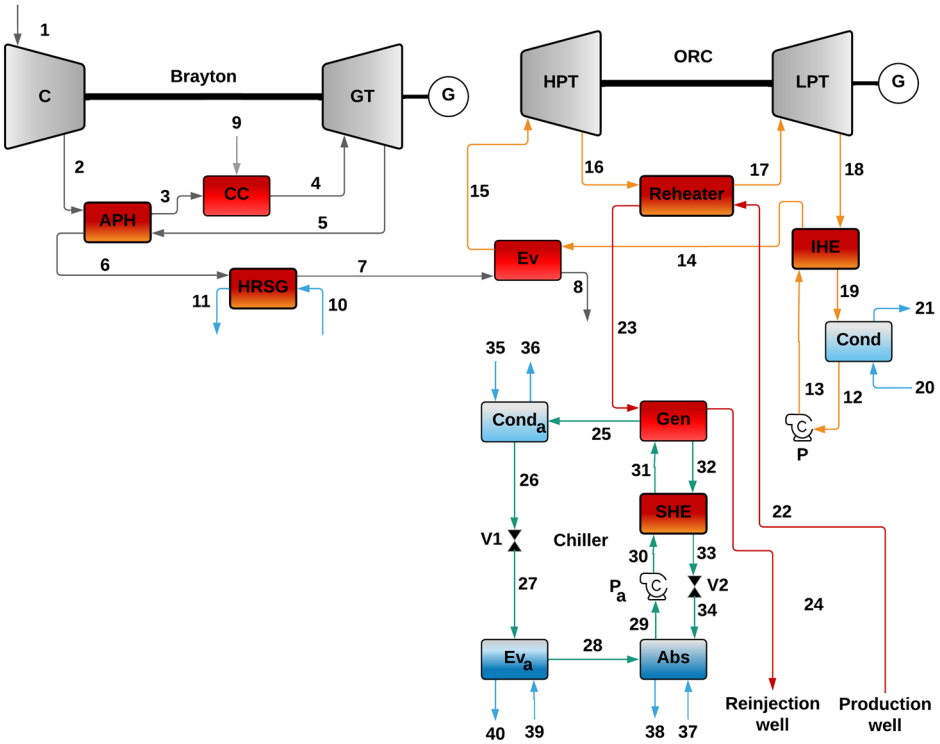

Figure 17. Schematic diagram of the hybrid ORC proposed by Pashapour et al. [142]. The different colors in Figure represent the different temperature levels in the cycle for thermal components.

Sharifishourabi and Chadegani [142] modeled a system for the production of cooling, hot water, heating, hydrogen, and power, simultaneously. The system included an ORC, a triple-effect ACS, a dehumidification system, and an electrolyzer. These components were driven by solar energy. The system reached an EUF of 0.39, a COP equal to 1.34, and energy and exergy efficiencies of 14.4% and 26%, respectively. Lee et al. [143] proposed the integration of an ORC with direct expansion and a proton-exchange membrane fuel cell (PEMFC) for power production in a liquid hydrogen-fueled ship. The authors analyzed the cycle, and the assessment results showed that the proposed system can achieve up to 221 kW of additional power, achieving energy and exergy efficiencies of up to 40.5% and 43.5%, respectively. The authors also found that the best working fluid for the considered application was propane.

Geng et al. [144] and Wang et al. [145] analyzed a G-ORC integrated into a desalination system. The variation in the zeotropic mixture composition could significantly improve the net power and the thermal efficiency of the ORC. The highest thermal exergy efficiencies were 13.3% and 51.5%, respectively.

Gholamian et al. [146] optimized a hybrid system integrating a basic G-ORC and a proton-exchange membrane electrolyzer to produce power and hydrogen simultaneously. Among others, the R114 was the best fluid. The maximum exergy efficiency was 21.9%, which was 12.7% higher than that obtained using just the basic ORC. Recently, Azad et al. [147], analyzed the integration of a two-stage in-series ORC and a fuel cell. This cycle utilized a PEMFC for electricity generation, an ORC with zeotropic mixtures for power production, and a thermoelectric generator instead of a condenser in the ORC as a heat recuperator used to produce electricity and minimize heat loss. It was found that this configuration can improve the overall exergy efficiency by 1.9%.

Kaşka et al. [148] presented a cycle integrating a G-ORC, a CCS, and a Claude cycle. The ORC was used to produce the electricity to drive the refrigeration cycle, which was

used in turn to produce the cold necessary to liquefy the hydrogen through the Claude cycle. The system was modeled using R600, R600a, R123, R245fa, and R141b. It was reported that the hydrogen liquefaction cost was 39.7% lower than values reported in the literature using traditional methods. Ganjehsarabi [149] proposed a system for the same purposes, but integrating a G-ORC coupled to a proton-exchange membrane electrolyzer. The exergy efficiencies were around 40% with the proposed fluids. Han et al. [150] also proposed a system for the simultaneous production of power and hydrogen. The system consisted of a steam turbine, an ORC, and a proton-exchange membrane electrolyzer. The maximum energy and exergy efficiencies were 18.96% and 57.24%, respectively. They were considerably higher than those reported by Ganjehsarabi [149], but required higher geothermal brine temperatures. Cao et al. [151] proposed another system for hydrogen production consisting of an electrolyzer fuel cell and a two-stage ORC. The highest energy and exergy efficiencies were 12.2% and 24.7%, respectively. The minimum electricity production cost was 36.6 USD/GJ. Recently, Fallah et al. [152], reported an exergy analysis for a hybrid cycle combining a supercritical CO_2 system coupled to an ORC as the bottoming cycle. The avoidable and unavoidable irreversibilities were determined and accounted for. The components where the highest irreversibilities took place were identified, as well as the avoidable part of irreversibility for each one. Thus, the authors determined the priority components that should be modified to reduce the overall exergy destruction.

Discussion of Hybrid Systems

Regarding the systems designed to produce only power, the best efficiency (19.2%) was achieved with the ORC integrated into a Brayton cycle [125], but requiring very high temperatures.

Among the systems integrating ORCs and cooling systems, the best was the one proposed by Wang et al. [132], using an eject-compressor cooling system. This system achieved an exergy efficiency of 59.16% operating at 190 °C, and was followed by the one proposed by Javanshir et al. [140], reaching a value of 57.9%.

With respect to the systems for producing three or more useful outputs, the one with the highest exergy efficiency was the one proposed by Han et al. [150], achieving an exergy efficiency of 57.1%; however, for the same purposes, the system proposed by Kaska et al. [148] reached the lowest LCOE, of 0.0247 USD/kWh.

7. Conclusions

Currently, there is great interest in studying and developing ORCs. Many studies have modeled them using a great variety of fluids, operating conditions, and configurations, from basic to advanced cycles; however, by contrast, the reported experimental studies number just a few. Other studies have proposed a variety of two-stage configurations to improve the performance parameters. Also, many hybrid cycles have combined ORCs with other technologies such as gas or steam turbines, cooling systems, or electrolyzers, to produce very interesting combinations of useful effects.

For theoretical studies, at temperatures below 120 °C, the highest thermal efficiencies were achieved with R123, R1233zd(E), R134a, R600, R290, R1234yf, and R245fa, while at higher temperatures, benzene, methanol, toluene, and cyclohexane were the best fluids. From the economic point of view, the best fluids were R1234yf and cyclohexane, but from the environmental perspective, R600, R601, R123, and R134a were the most convenient at low heat source temperatures, while toluene was better at high heat source temperatures.

Regarding the theoretical single-stage cycles, the most efficient were both the recuperative and regenerative configurations, achieving thermal efficiencies up to 15% higher than those of the basic cycles. It was also found that supercritical cycles could produce up to 20% more power than subcritical cycles. As for the two-stage configurations, it is concluded that it is not feasible to objectively compare them, since these studies were performed considering different working fluids and operating conditions; however, in most of them, the authors reported that thermal efficiencies and power could be, respectively, up

to 20% and 44% higher than in single-stage cycles. On the other hand, the most efficient hybrid systems were those integrating Brayton cycles, although they require operating temperatures around 300 °C higher than systems integrating a steam turbine.

Some of the recent studies have focused on integrating ORC into other conventional cycles, such as binary geothermal or Bryton cycles, while others have integrated new components into the basic cycle to make it more efficient, or with polygeneration purposes. It was found that most of the studies on new cycles are theoretical, and none of them report the performance of modified cycles apart from the regenerative or recuperative, which shows there is an important gap between the proposed theoretical configurations and the development of experimental prototypes. Nevertheless, this gap is, in general, usual in the development of energy technologies, and thus it is expected that in the forthcoming years new prototypes will emerge, based on some of the new theoretical cycles proposed.

8. Future Directions

Based on the observed trends, future research on ORC could lean toward the trends mentioned below:

1. Simulation of dynamic systems: Some recent studies on energy systems, including ORCs, have proposed dynamic models that consider the transient behavior of the main operating parameters, showing a more realistic performance than the steady-state models.
2. Experimental validation: to date, the vast majority of studies on ORC have not been validated experimentally, which results in a huge number of cycles with attractive performance parameters, but without certainty regarding their technical or economic viability. A major experimental research effort should be carried out in the short and medium term.
3. Characterization of working fluids: To move towards new possibilities in terms of working fluids, it is fundamental that there should shortly be more research on the definition of the thermophysical properties of new working fluids, particularly for zeotropic mixtures, under the conditions of interest for the ORC.
4. Cogeneration systems: the analyses of current hybrid structures mostly predict a better performance of the systems in which the ORCs are integrated. Future proposals for systems producing several useful effects, particularly those of an empirical nature, should be encouraged.
5. Multi-objective optimization: the vast majority of optimization analyses have focused on energy and economic parameters; however, they leave aside environmental aspects. It is expected that the studies on new power cycles will soon be complemented, including an environmental approach (life cycle analyses or assessment of direct/indirect emissions).
6. Supercritical ORC: some studies [93] indicate that supercritical cycles can be more efficient than subcritical ones in certain conditions (low-temperature heat sources). Thus, research efforts should be addressed to investigate the actual potential of these systems.
7. Cleaner production: it is expected that the growing operation of ORCs driven by clean energy sources such as geothermal, solar, and biomass will be maintained, or even those driven by waste heat of an industrial nature or any process where the integration of an ORC has the potential to improve overall energy efficiency.

Some other authors [153] consider that reversible ORC heat pump systems also represent an additional field of interest to work in, as a key solution to waste heat recovery, together with thermal and electrical energy storage.

Author Contributions: Conceptualization, W.R.; methodology, W.R.; investigation, J.C.J.-G., A.R., A.P.-R. and W.R.; writing—original draft preparation, A.R., J.C.J.-G. and A.P.-R.; writing—review and editing, J.C.J.-G.; visualization, A.P.-R. and J.C.J.-G.; supervision, W.R.; project administration, W.R. All authors have read and agreed to the published version of the manuscript.

Funding: This research received no external funding.

Data Availability Statement: No new data were created or analyzed in this study. Data sharing is not applicable to this article.

Conflicts of Interest: The authors declare no conflict of interest.

Nomenclature

ACS	absorption cooling system
CCS	compression cooling system
DS	dehumidification system
ECS	ejector cooling system
ExD	exergy destruction
Exp	expander
COP	coefficient of performance
G	generator
HPE	high-pressure evaporator
HPT	high-pressure turbine
HS	heat source
LPE	low-pressure evaporator
LPT	low-pressure turbine
LCOE	levelized cost of energy
ORC	organic Rankine cycle
PBP	payback period
SP	single-pressure
TP	two-pressure

References

1. IEA. *Global Energy Review: CO_2 Emissions in 2021*; IEA: Paris, France, 2022.
2. BCS. *Waste Heat Recovery: Technology and Opportunities in U. S. Industry*; BCS, Inc.: Laurel, MD, USA, 2008.
3. Thekdi, A.; Nimbalkar, S.U. *Industrial Waste Heat Recovery-Potential Applications, Available Technologies and Crosscutting R&D Opportunities*; Oak Ridge National Lab (ORNL): Oak Ridge, TN, USA, 2015.
4. Park, B.-S.; Usman, M.; Imran, M.; Pesyridis, A. Review of Organic Rankine Cycle experimental data trends. *Energy Convers. Manag.* **2018**, *173*, 679–691. [CrossRef]
5. Tartière, T.; Astolfi, M. A world overview of the organic Rankine cycle market. *Energy Procedia* **2017**, *129*, 2–9. [CrossRef]
6. Pethurajan, V.; Sivan, S.; Joy, G.C. Issues, comparisons, turbine selections and applications–An overview in organic Rankine cycle. *Energy Convers. Manag.* **2018**, *166*, 474–488. [CrossRef]
7. Ahmadi, A.; Assad ME, H.; Jamali, D.H.; Kumar, R.; Li, Z.X.; Salameh, T.; Al-Shabi, M.; Ehyaei, M.A. Applications of geothermal organic Rankine Cycle for electricity production. *J. Clean. Prod.* **2020**, *274*, 122950. [CrossRef]
8. Haghighi, A.; Pakatchian, M.R.; Assad, M.E.H.; Duy, V.N.; Alhuyi Nazari, M. A review on geothermal Organic Rankine cycles: Modeling and optimization. *J. Therm. Anal. Calorim.* **2021**, *144*, 1799–1814. [CrossRef]
9. Wieland, C.; Schifflechner, C.; Dawo, F.; Astolfi, M. The organic Rankine cycle power systems market: Recent developments and future perspectives. *Appl. Therm. Eng.* **2023**, *224*, 119980. [CrossRef]
10. Nondy, J.; Gogoi, T.K. Exergoeconomic investigation and multi-objective optimization of different ORC configurations for waste heat recovery: A comparative study. *Energy Convers. Manag.* **2021**, *245*, 114593. [CrossRef]
11. Zhang, X.; Zhang, C.; He, M.; Wang, J. Selection and evaluation of dry and isentropic organic working fluids used in organic Rankine cycle based on the turning point on their saturated vapor curves. *J. Therm. Sci.* **2019**, *28*, 643–658. [CrossRef]
12. Györke, G.; Groniewsky, A.; Imre, A.R. A simple method of finding new dry and isentropic working fluids for organic rankine cycle. *Energies* **2019**, *12*, 480. [CrossRef]
13. Imre, A.R.; Kustán, R.; Groniewsky, A. Thermodynamic selection of the optimal working fluid for organic Rankine cycles. *Energies* **2019**, *12*, 2028. [CrossRef]
14. Györke, G.; Deiters, U.K.; Groniewsky, A.; Lassu, I.; Imre, A.R. Novel classification of pure working fluids for Organic Rankine Cycle. *Energy* **2018**, *145*, 288–300. [CrossRef]
15. Wang, E.; Zhang, M.; Meng, F.; Zhang, H. Zeotropic working fluid selection for an organic Rankine cycle bottoming with a marine engine. *Energy* **2022**, *243*, 123097. [CrossRef]
16. Blondel, Q.; Tauveron, N.; Lhermet, G.; Caney, N. Zeotropic mixtures study in plate heat exchangers and ORC systems. *Appl. Therm. Eng.* **2023**, *219*, 119418. [CrossRef]

17. Yang, L.; Gong, M.; Guo, H.; Dong, X.; Shen, J.; Wu, J. Effects of critical and boiling temperatures on system performance and fluid selection indicator for low temperature organic Rankine cycles. *Energy* **2016**, *109*, 830–844. [CrossRef]
18. Li, J.; Alvi, J.Z.; Pei, G.; Su, Y.; Li, P.; Gao, G.; Ji, J. Modelling of organic Rankine cycle efficiency with respect to the equivalent hot side temperature. *Energy* **2016**, *115*, 668–683. [CrossRef]
19. Dai, B.; Zhu, K.; Wang, Y.; Sun, Z.; Liu, Z. Evaluation of organic Rankine cycle by using hydrocarbons as working fluids: Advanced exergy and advanced exergoeconomic analyses. *Energy Convers. Manag.* **2019**, *197*, 111876. [CrossRef]
20. Luo, X.; Wang, Y.; Liang, J.; Qi, J.; Su, W.; Yang, Z.; Chen, J.; Wang, C.; Chen, Y. Improved correlations for working fluid properties prediction and their application in performance evaluation of sub-critical Organic Rankine Cycle. *Energy* **2019**, *174*, 122–137. [CrossRef]
21. Fan, W.; Han, Z.; Li, P.; Jia, Y. Analysis of the thermodynamic performance of the organic Rankine cycle (ORC) based on the characteristic parameters of the working fluid and criterion for working fluid selection. *Energy Convers. Manag.* **2020**, *211*, 112746. [CrossRef]
22. Zhang, X.; Li, Y. An examination of super dry working fluids used in regenerative organic Rankine cycles. *Energy* **2023**, *263*, 125931. [CrossRef]
23. Bianchi, M.; Branchini, L.; De Pascale, A.; Melino, F.; Ottaviano, S.; Peretto, A.; Torricelli, N. Performance and total warming impact assessment of pure fluids and mixtures replacing HFCs in micro-ORC energy systems. *Appl. Therm. Eng.* **2022**, *203*, 117888. [CrossRef]
24. Bahrami, M.; Pourfayaz, F.; Kasaeian, A. Low global warming potential (GWP) working fluids (WFs) for Organic Rankine Cycle (ORC) applications. *Energy Rep.* **2022**, *8*, 2976–2988. [CrossRef]
25. Nurhilal, O.; Mulyana, C.; Suhendi, N.; Sapdiana, D. The simulation of organic rankine cycle power plant with n-pentane working fluid. In *AIP Conference Proceedings*; AIP Publishing LLC: Long Island, NY, USA, 2016; p. 040003. [CrossRef]
26. Herath, H.M.D.P.; Wijewardane, M.A.; Ranasinghe, R.A.C.P.; Jayasekera, J.G.A.S. Working fluid selection of Organic Rankine Cycles. *Energy Rep.* **2020**, *6*, 680–686. [CrossRef]
27. Yadav, K.; Sircar, A. Selection of working fluid for low enthalpy heat source Organic Rankine Cycle in Dholera, Gujarat, India. *Case Stud. Therm. Eng.* **2019**, *16*, 100553. [CrossRef]
28. Wang, H.; Li, H.; Wang, L.; Bu, X. Thermodynamic Analysis of Organic Rankine Cycle with Hydrofluoroethers as Working Fluids. *Energy Procedia.* **2017**, *105*, 1889–1894. [CrossRef]
29. Sakhrieha, A.; Shreimb, W.; Fakhruldeenb, H.; Hasanb, H.; Al-Salaymeh, A. Combined Solar-Geothermal Power Generation using Organic Rankine Cycle. *Jordan J. Mech. Ind. Eng.* **2016**, *10*, 1–9.
30. Senturk Acar, M.; Arslan, O. Energy and exergy analysis of solar energy-integrated, geothermal energy-powered Organic Rankine Cycle. *J. Therm. Anal. Calorim.* **2019**, *137*, 659–666. [CrossRef]
31. Bademlioglu, A.H. Exergy analysis of the organic rankine cycle based on the pinch point temperature difference. *J. Therm. Eng.* **2019**, *5*, 157–165. [CrossRef]
32. Yamankaradeniz, N.; Bademlioglu, A.H.; Kaynakli, O. Performance Assessments of Organic Rankine Cycle With Internal Heat Exchanger Based on Exergetic Approach. *J. Energy Resour. Technol.* **2018**, *140*, 102001. [CrossRef]
33. Invernizzi, C.; Binotti, M.; Bombarda, P.; Di Marcoberardino, G.; Iora, P.; Manzolini, G. Water Mixtures as Working Fluids in Organic Rankine Cycles. *Energies* **2019**, *12*, 2629. [CrossRef]
34. Sun, Z.; Huang, Y.; Tian, N.; Lin, K. Performance improvement of ORC by breaking the barrier of ambient pressure. *Energy* **2023**, *262*, 125408. [CrossRef]
35. de Neto, R.O.; Sotomonte, C.A.R.; Coronado, C.J.R. Off-design model of an ORC system for waste heat recovery of an internal combustion engine. *Appl. Therm. Eng.* **2021**, *195*, 117188. [CrossRef]
36. Ping, X.; Yang, F.; Zhang, H.; Xing, C.; Yu, M.; Wang, Y. Investigation and multi-objective optimization of vehicle engine-organic Rankine cycle (ORC) combined system in different driving conditions. *Energy* **2023**, *263*, 125672. [CrossRef]
37. Khosravi, A.; Syri, S.; Zhao, X.; Assad, M.E.H. An artificial intelligence approach for thermodynamic modeling of geothermal based-organic Rankine cycle equipped with solar system. *Geothermics* **2019**, *80*, 138–154. [CrossRef]
38. Sun, J.; Liu, Q.; Duan, Y. Effects of evaporator pinch point temperature difference on thermo-economic performance of geothermal organic Rankine cycle systems. *Geothermics* **2018**, *75*, 249–258. [CrossRef]
39. Mustapic, N.; Brkic, V.; Kerin, M. Subcritical organic ranking cycle based geothermal power plant thermodynamic and economic analysis. *Therm. Sci.* **2018**, *22*, 2137–2150. [CrossRef]
40. Kyriakarakos, G.; Ntavou, E.; Manolakos, D. Investigation of the Use of Low Temperature Geothermal Organic Rankine Cycle Engine in an Autonomous Polygeneration Microgrid. *Sustainability* **2020**, *12*, 10475. [CrossRef]
41. Usman, M.; Imran, M.; Yang, Y.; Lee, D.H.; Park, B.-S. Thermo-economic comparison of air-cooled and cooling tower based Organic Rankine Cycle (ORC) with R245fa and R1233zde as candidate working fluids for different geographical climate conditions. *Energy* **2017**, *123*, 353–366. [CrossRef]
42. Oyewunmi, O.; Markides, C. Thermo-Economic and Heat Transfer Optimization of Working-Fluid Mixtures in a Low-Temperature Organic Rankine Cycle System. *Energies* **2016**, *9*, 448. [CrossRef]
43. Yaïci, W.; Entchev, E.; Talebizadehsardari, P.; Longo, M. Thermodynamic, Economic and Sustainability Analysis of Solar Organic Rankine Cycle System with Zeotropic Working Fluid Mixtures for Micro-Cogeneration in Buildings. *Appl. Sci.* **2020**, *10*, 7925. [CrossRef]

44. Baral, S. Experimental and Techno-Economic Analysis of Solar-Geothermal Organic Rankine Cycle Technology for Power Generation in Nepal. *Int. J. Photoenergy* **2019**, *2019*, 5814265. [CrossRef]
45. Ergun, A.; Ozkaymak, M.; Aksoy Koc, G.; Ozkan, S.; Kaya, D. Exergoeconomic analysis of a geothermal organic Rankine cycle power plant using the SPECO method. *Environ. Prog. Sustain. Energy* **2017**, *36*, 936–942. [CrossRef]
46. Oyekale, J.; Petrollese, M.; Heberle, F.; Brüggemann, D.; Cau, G. Exergetic and integrated exergoeconomic assessments of a hybrid solar-biomass organic Rankine cycle cogeneration plant. *Energy Convers. Manag.* **2020**, *215*, 112905. [CrossRef]
47. Wang, S.; Liu, C.; Zhang, S.; Li, Q.; Huo, E. Multi-objective optimization and fluid selection of organic Rankine cycle (ORC) system based on economic-environmental-sustainable analysis. *Energy Convers. Manag.* **2022**, *254*, 115238. [CrossRef]
48. Zhang, H.; Guan, X.; Ding, Y.; Liu, C. Emergy analysis of Organic Rankine Cycle (ORC) for waste heat power generation. *J. Clean. Prod.* **2018**, *183*, 1207–1215. [CrossRef]
49. Li, G. Organic Rankine cycle environmental impact investigation under various working fluids and heat domains concerning refrigerant leakage rates. *Int. J. Environ. Sci. Technol.* **2019**, *16*, 431–450. [CrossRef]
50. Yi, Z.; Luo, X.; Yang, Z.; Wang, C.; Chen, J.; Chen, Y.; Ponce-Ortega, J.M. Thermo-economic-environmental optimization of a liquid separation condensation-based organic Rankine cycle driven by waste heat. *J. Clean. Prod.* **2018**, *184*, 198–210. [CrossRef]
51. Pintoro, A.; Ambarita, H.; Nur, T.B.; Napitupulu, F.H. Performance analysis of low temperature heat source of organic Rankine cycle for geothermal application. *IOP Conf. Ser. Mater. Sci. Eng.* **2018**, *308*, 012026. [CrossRef]
52. Boydak, O.; Ekmekci, I.; Yilmaz, M.; Koten, H. Thermodynamic investigation of organic Rankine cycle energy recovery system and recent studies. *Therm. Sci.* **2018**, *22*, 2679–2690. [CrossRef]
53. Lin, C.H.; Hsu, P.P.; He, Y.L.; Shuai, Y.; Hung, T.C.; Feng, Y.Q.; Chang, Y.H. Investigations on experimental performance and system behavior of 10 kW organic Rankine cycle using scroll-type expander for low-grade heat source. *Energy* **2019**, *177*, 94–105. [CrossRef]
54. Prasetyo, T.; Surindra, M.D.; Caesarendra, W.; Taufik Glowacz, A.; Irfan, M.; Glowacz, W. Influence of Superheated Vapour in Organic Rankine Cycles with Working Fluid R123 Utilizing Low-Temperature Geothermal Resources. *Symmetry* **2020**, *12*, 1463. [CrossRef]
55. Alshammari, F.; Elashmawy, M.; Bechir Ben Hamida, M. Effects of working fluid type on powertrain performance and turbine design using experimental data of a 7.25ℓ heavy-duty diesel engine. *Energy Convers. Manag.* **2021**, *231*, 113828. [CrossRef]
56. Abbas, W.K.A.; Linnemann, M.; Baumhögger, E.; Vrabec, J. Experimental study of two cascaded organic Rankine cycles with varying working fluids. *Energy Convers. Manag.* **2021**, *230*, 113818. [CrossRef]
57. Tumen Ozdil, N.F.; Segmen, M.R. Investigation of the effect of the water phase in the evaporator inlet on economic performance for an Organic Rankine Cycle (ORC) based on industrial data. *Appl. Therm. Eng.* **2016**, *100*, 1042–1051. [CrossRef]
58. Surindra, M.; Caesarendra, W.; Prasetyo, T.; Mahlia, T.; Taufik. Comparison of the Utilization of 110 °C and 120 °C Heat Sources in a Geothermal Energy System Using Organic Rankine Cycle (ORC) with R245fa, R123, and Mixed-Ratio Fluids as Working Fluids. *Processes* **2019**, *7*, 113. [CrossRef]
59. Özkaraca, O.; Keçebaş, P.; Demircan, C.; Keçebaş, A. Thermodynamic Optimization of a Geothermal- Based Organic Rankine Cycle System Using an Artificial Bee Colony Algorithm. *Energies* **2017**, *10*, 1691. [CrossRef]
60. Ali, M.; Khan, T.; Hajri, E. A Computer program for working fluid selection of low temperature organic Rankine cycle. In *ASME Power Conference*; American Society of Mechanical Engineers: New York, NY, USA, 2015. [CrossRef]
61. Li, G. Organic Rankine cycle performance evaluation and thermoeconomic assessment with various applications part I: Energy and exergy performance evaluation. *Renew. Sustain. Energy Rev.* **2016**, *53*, 477–499. [CrossRef]
62. Unverdi, M.; Cerci, Y. Thermodynamic analysis and performance improvement of Irem geothermal power plant in Turkey: A case study of organic Rankine cycle. *Environ. Prog. Sustain. Energy* **2018**, *37*, 1523–1539. [CrossRef]
63. Moradi, R.; Habib, E.; Bocci, E.; Cioccolanti, L. Component-Oriented Modeling of a Micro-Scale Organic Rankine Cycle System for Waste Heat Recovery Applications. *Appl. Sci.* **2021**, *11*, 1984. [CrossRef]
64. Peris, B.; Navarro-Esbrí, J.; Molés, F.; Mota-Babiloni, A. Experimental study of an ORC (organic Rankine cycle) for low grade waste heat recovery in a ceramic industry. *Energy* **2015**, *85*, 534–542. [CrossRef]
65. Peris, B.; Navarro-Esbrí, J.; Mateu-Royo, C.; Mota-Babiloni, A.; Molés, F.; Gutiérrez-Trashorras, A.J.; Amat-Albuixech, M. Thermo-economic optimization of small-scale Organic Rankine Cycle: A case study for low-grade industrial waste heat recovery. *Energy* **2020**, *213*, 118898. [CrossRef]
66. Landelle, A.; Tauveron, N.; Haberschill, P.; Revellin, R.; Colasson, S. Performance Evaluation and Comparison of Experimental Organic Rankine Cycle Prototypes from Published Data. *Energy Procedia.* **2017**, *105*, 1706–1711. [CrossRef]
67. Eyidogan, M.; Canka Kilic, F.; Kaya, D.; Coban, V.; Cagman, S. Investigation of Organic Rankine Cycle (ORC) technologies in Turkey from the technical and economic point of view. *Renew. Sustain. Energy Rev.* **2016**, *58*, 885–895. [CrossRef]
68. Zhai, H.; An, Q.; Shi, L.; Lemort, V.; Quoilin, S. Categorization and analysis of heat sources for organic Rankine cycle systems. *Renew. Sustain. Energy Rev.* **2016**, *64*, 790–805. [CrossRef]
69. Algieri, A.; Šebo, J. Energetic investigation of organic rankine cycles (ORCs) for the exploitation of low-temperature geothermal sources–a possible application in Slovakia. *Procedia Comput. Sci.* **2017**, *109*, 833–840. [CrossRef]
70. Canbolat, A.S.; Bademlioglu, A.H.; Kaynakli, O. A modeling of electricity generation by using geothermal assisted organic Rankine cycle with internal heat recovery. *Energy Sources Part A Recovery Util. Environ. Eff.* **2023**, *45*, 212–228. [CrossRef]

71. Zhang, C.; Fu, J.; Yuan, P.; Liu, J. Guidelines for optimal selection of subcritical low-temperature geothermal organic Rankine cycle configuration considering reinjection temperature limits. *Energies* **2018**, *11*, 2878. [CrossRef]
72. Proctor, M.; Yu, W.; Kirkpatrick, R.; Young, B. Dynamic modelling and validation of a commercial scale geothermal organic rankine cycle power plant. *Energies* **2016**, *61*, 63–74. [CrossRef]
73. Uusitalo, A.; Honkatukia, J.; Turunen-Saaresti, T.; Grönman, A. Thermodynamic evaluation on the effect of working fluid type and fluids critical properties on design and performance of Organic Rankine Cycles. *J. Clean. Prod.* **2018**, *188*, 253–263. [CrossRef]
74. Pezzuolo, A.; Benato, A.; Stoppato, A.; Mirandola, A. The ORC-PD: A versatile tool for fluid selection and Organic Rankine Cycle unit design. *Energy* **2016**, *102*, 605–620. [CrossRef]
75. Agromayor, R.; Nord, L.O. Fluid selection and thermodynamic optimization of organic Rankine cycles for waste heat recovery applications. *Energy Procedia* **2017**, *129*, 527–534. [CrossRef]
76. Huster, W.R.; Bongartz, D.; Mitsos, A. Deterministic global optimization of the design of a geothermal organic rankine cycle. *Energy Procedia* **2017**, *129*, 50–57. [CrossRef]
77. Preißinger, M.; Brüggemann, D. Thermoeconomic evaluation of modular organic Rankine cycles for waste heat recovery over a broad range of heat source temperatures and capacities. *Energies* **2017**, *10*, 269. [CrossRef]
78. Heberle, F.; Hofer, M.; Brüggemann, D. A Retrofit for Geothermal Organic Rankine Cycles based on Concentrated Solar Thermal Systems. *Energy Procedia* **2017**, *129*, 692–699. [CrossRef]
79. Heberle, F.; Hofer, M.; Ürlings, N.; Schröder, H.; Anderlohr, T.; Brüggemann, D. Techno-economic analysis of a solar thermal retrofit for an air-cooled geothermal Organic Rankine Cycle power plant. *Renew. Energy* **2017**, *113*, 494–502. [CrossRef]
80. Stoppato, A.; Benato, A. Life Cycle Assessment of a Commercially Available Organic Rankine Cycle Unit Coupled with a Biomass Boiler. *Energies* **2020**, *13*, 1835. [CrossRef]
81. Lu, J.; Zhang, J.; Chen, S.; Pu, Y. Analysis of organic Rankine cycles using zeotropic mixtures as working fluids under different restrictive conditions. *Energy Convers. Manag.* **2016**, *126*, 704–716. [CrossRef]
82. Tiwari, D.; Sherwani, A.F.; Asjad, M.; Arora, A. Grey relational analysis coupled with principal component analysis for optimization of the cyclic parameters of a solar-driven organic Rankine cycle. *Grey Syst.* **2017**, *7*, 218–235. [CrossRef]
83. Van Erdeweghe, S.; Van Bael, J.; Laenen, B.; D'haeseleer, W. Design and off-design optimization procedure for low-temperature geothermal organic Rankine cycles. *Appl. Energy* **2019**, *242*, 716–731. [CrossRef]
84. Imran, M.; Usman, M.; Park, B.S.; Yang, Y. Comparative assessment of Organic Rankine Cycle integration for low temperature geothermal heat source applications. *Energy* **2016**, *102*, 473–490. [CrossRef]
85. Wang, Y.Z.; Zhao, J.; Wang, Y.; An, Q.S. Multi-objective optimization and grey relational analysis on configurations of organic Rankine cycle. *Appl. Therm. Eng.* **2017**, *114*, 1355–1363. [CrossRef]
86. Li, G. Organic Rankine cycle performance evaluation and thermoeconomic assessment with various applications part II: Economic assessment aspect. *Renew. Sustain. Energy Rev.* **2016**, *64*, 490–505. [CrossRef]
87. Yang, M.H.; Yeh, R.H. Economic performances optimization of an organic Rankine cycle system with lower global warming potential working fluids in geothermal application. *Renew. Energy* **2016**, *85*, 1201–1213. [CrossRef]
88. Zhar, R.; Allouhi, A.; Jamil, A.; Lahrech, K. A comparative study and sensitivity analysis of different ORC configurations for waste heat recovery. *Case Stud. Therm. Eng.* **2021**, *28*, 101608. [CrossRef]
89. Javed, S.; Tiwari, A.K. Performance assessment of different Organic Rankine Cycle (ORC) configurations driven by solar energy. *Process Saf. Environ. Prot.* **2023**, *171*, 655–666. [CrossRef]
90. Liu, C.; Gao, T.; Zhu, J.; Xu, J. Performance Optimization and Economic Analysis of Geothermal Power Generation by Subcritical and Supercritical Organic Rankine Cycles. In *Turbo Expo: Power for Land, Sea, and Air*; American Society of Mechanical Engineers: New York, NY, USA, 2016; Volume 3. [CrossRef]
91. Manente, G.; Da Lio, L.; Lazzaretto, A. Influence of axial turbine efficiency maps on the performance of subcritical and supercritical Organic Rankine Cycle systems. *Energy* **2016**, *107*, 761–772. [CrossRef]
92. Chagnon-Lessard, N.; Mathieu-Potvin, F.; Gosselin, L. Geothermal power plants with maximized specific power output: Optimal working fluid and operating conditions of subcritical and transcritical Organic Rankine Cycles. *Geothermics* **2016**, *64*, 111–124. [CrossRef]
93. Moloney, F.; Almatrafi, E.; Goswami, D.Y. Working fluid parametric analysis for recuperative supercritical organic Rankine cycles for medium geothermal reservoir temperatures. *Renew. Energy* **2020**, *147*, 2874–2881. [CrossRef]
94. Erdogan, A.; Colpan, O. Performance assessment of shell and tube heat exchanger based subcritical and supercritical organic Rankine cycles. *Therm. Sci.* **2018**, *22*, 855–866. [CrossRef]
95. Lukawski, M.Z.; Tester, J.W.; Dipippo, R. Impact of molecular structure of working fluids on performance of organic Rankine cycles (ORCs). *Sustain. Energy Fuels* **2017**, *1*, 1098–1111. [CrossRef]
96. Song, C.; Gu, M.; Miao, Z.; Liu, C.; Xu, J. Effect of fluid dryness and critical temperature on trans-critical organic Rankine cycle. *Energy* **2019**, *174*, 97–109. [CrossRef]
97. Wang, X.; Levy, E.K.; Pan, C.; Romero, C.E.; Banerjee, A.; Rubio-Maya, C.; Pan, L. Working fluid selection for organic Rankine cycle power generation using hot produced supercritical CO_2 from a geothermal reservoir. *Appl. Therm. Eng.* **2019**, *149*, 1287–1304. [CrossRef]
98. Cakici, D.M.; Erdogan, A.; Colpan, C.O. Thermodynamic performance assessment of an integrated geothermal powered supercritical regenerative organic Rankine cycle and parabolic trough solar collectors. *Energy* **2017**, *120*, 306–319. [CrossRef]

99. Sun, Q.; Wang, Y.; Cheng, Z.; Wang, J.; Zhao, P.; Dai, Y. Thermodynamic Optimization of a Double-pressure Organic Rankine Cycle Driven by Geothermal Heat Source. *Energy Procedia.* **2017**, *129*, 591–598. [CrossRef]
100. Sun, Q.; Wang, Y.; Cheng, Z.; Wang, J.; Zhao, P.; Dai, Y. Thermodynamic and economic optimization of a double-pressure organic Rankine cycle driven by low-temperature heat source. *Renew. Energy* **2020**, *147*, 2822–2832. [CrossRef]
101. Manente, G.; Lazzaretto, A.; Bonamico, E. Design guidelines for the choice between single and dual pressure layouts in organic Rankine cycle (ORC) systems. *Energy* **2017**, *123*, 413–431. [CrossRef]
102. Wang, S.; Liu, C.; Zhang, C.; Xu, X.; Li, Q. Thermo-economic evaluations of dual pressure organic Rankine cycle (DPORC) driven by geothermal heat source. *J. Renew. Sustain. Energy* **2018**, *10*, 063901. [CrossRef]
103. Fontalvo, A.; Solano, J.; Pedraza, C.; Bula, A.; Quiroga, A.G.; Padilla, R.V. Energy, Exergy and Economic Evaluation Comparison of Small-Scale Single and Dual Pressure Organic Rankine Cycles Integrated with Low-Grade Heat Sources. *Entropy* **2017**, *19*, 476. [CrossRef]
104. Braimakis, K.; Karellas, S. Energetic optimization of regenerative Organic Rankine Cycle (ORC) configurations. *Energy Convers. Manag.* **2018**, *159*, 353–370. [CrossRef]
105. Braimakis, K.; Karellas, S. Exergetic optimization of double stage Organic Rankine Cycle (ORC). *Energy* **2018**, *149*, 296–313. [CrossRef]
106. Liu, G.; Wang, Q.; Xu, J.; Miao, Z. Exergy Analysis of Two-Stage Organic Rankine Cycle Power Generation System. *Entropy* **2021**, *23*, 43. [CrossRef]
107. Li, T.; Yuan, Z.; Li, W.; Yang, J.; Zhu, J. Strengthening mechanisms of two-stage evaporation strategy on system performance for organic Rankine cycle. *Energy* **2016**, *101*, 532–540. [CrossRef]
108. Li, T.L.; Yuan, Z.H.; Xu, P.; Zhu, J.L. Entransy dissipation/loss-based optimization of two-stage organic Rankine cycle (TSORC) with R245fa for geothermal power generation. *Sci. China Technol. Sci.* **2016**, *59*, 1524–1536. [CrossRef]
109. Wang, J.; Xu, P.; Li, T.; Zhu, J. Performance enhancement of organic Rankine cycle with two-stage evaporation using energy and exergy analyses. *Geothermics* **2017**, *65*, 126–134. [CrossRef]
110. Li, J.; Ge, Z.; Duan, Y.; Yang, Z.; Liu, Q. Parametric optimization and thermodynamic performance comparison of single-pressure and dual-pressure evaporation organic Rankine cycles. *Appl. Energy* **2018**, *217*, 409–421. [CrossRef]
111. Wang, M.; Chen, Y.; Liu, Q.; Yuanyuan, Z. Thermodynamic and thermo-economic analysis of dual-pressure and single pressure evaporation organic Rankine cycles. *Energy Convers. Manag.* **2018**, *177*, 718–736. [CrossRef]
112. Kazemi, N.; Samadi, F. Thermodynamic, economic and thermo-economic optimization of a new proposed organic Rankine cycle for energy production from geothermal resources. *Energy Convers. Manag.* **2016**, *121*, 391–401. [CrossRef]
113. Samadi, F.; Kazemi, N. Exergoeconomic analysis of zeotropic mixture on the new proposed organic Rankine cycle for energy production from geothermal resources. *Renew. Energy.* **2020**, *152*, 1250–1265. [CrossRef]
114. Nami, H.; Nemati, A.; Jabbari Fard, F. Conventional and advanced exergy analyses of a geothermal driven dual fluid organic Rankine cycle (ORC). *Appl. Therm. Eng.* **2017**, *122*, 59–70. [CrossRef]
115. Luo, X.; Huang, R.; Yang, Z.; Chen, J.; Chen, Y. Performance investigation of a novel zeotropic organic Rankine cycle coupling liquid separation condensation and multi-pressure evaporation. *Energy Convers. Manag.* **2018**, *161*, 112–127. [CrossRef]
116. Zhou, Y.; Li, S.; Sun, L.; Zhao, S.; Ashraf Talesh, S.S. Optimization and thermodynamic performance analysis of a power generation system based on geothermal flash and dual-pressure evaporation organic Rankine cycles using zeotropic mixtures. *Energy* **2020**, *194*, 116785. [CrossRef]
117. Surendran, A.; Seshadri, S. Design and performance analysis of a novel Transcritical Regenerative Series Two stage Organic Rankine Cycle for dual source waste heat recovery. *Energy* **2020**, *203*, 117800. [CrossRef]
118. Li, T.; Hu, X.; Wang, J.; Kong, X.; Liu, J.; Zhu, J. Performance improvement of two-stage serial organic Rankine cycle (TSORC) driven by dual-level heat sources of geothermal energy coupled with solar energy. *Geothermics* **2018**, *76*, 261–270. [CrossRef]
119. Heberle, F.; Schifflechner, C.; Brüggemann, D. Life cycle assessment of Organic Rankine Cycles for geothermal power generation considering low-GWP working fluids. *Geothermics* **2016**, *64*, 392–400. [CrossRef]
120. Sadeghi, M.; Nemati, A.; Ghavimi, A.; Yari, M. Thermodynamic analysis and multi-objective optimization of various ORC (organic Rankine cycle) configurations using zeotropic mixtures. *Energy* **2016**, *109*, 791–802. [CrossRef]
121. Chagnon-Lessard, N.; Mathieu-Potvin, F.; Gosselin, L. Optimal design of geothermal power plants: A comparison of single-pressure and dual-pressure organic Rankine cycles. *Geothermics* **2020**, *86*, 101787. [CrossRef]
122. Wang, Q.; Wang, J.; Li, T.; Meng, N. Techno-economic performance of two-stage series evaporation organic Rankine cycle with dual-level heat sources. *Appl. Therm. Eng.* **2020**, *171*, 115078. [CrossRef]
123. Wang, Z.; Xia, X.; Pan, H.; Zuo, Q.; Zhou, N.; Xie, B. Fluid selection and advanced exergy analysis of dual-loop ORC using zeotropic mixture. *Appl. Therm. Eng.* **2021**, *185*, 116423. [CrossRef]
124. Najjar, Y.S.H.; Qatramez, A.E. Energy utilisation in a combined geothermal and organic Rankine power cycles. *Int. J. Sustain. Energy* **2019**, *38*, 831–848. [CrossRef]
125. Matuszewska, D.; Olczak, P. Evaluation of Using Gas Turbine to Increase Efficiency of the Organic Rankine Cycle (ORC). *Energies* **2020**, *13*, 1499. [CrossRef]
126. Yağlı, H.; Koç, Y.; Kalay, H. Optimisation and exergy analysis of an organic Rankine cycle (ORC) used as a bottoming cycle in a cogeneration system producing steam and power. *Sustain. Energy Technol. Assess.* **2021**, *44*, 100985. [CrossRef]

127. Hassani Mokarram, N.; Mosaffa, A.H. Investigation of the thermoeconomic improvement of integrating enhanced geothermal single flash with transcritical organic Rankine cycle. *Energy Convers. Manag.* **2020**, *213*, 112831. [CrossRef]
128. Li, Z.; Li, W.; Xu, B. Optimization of mixed working fluids for a novel trigeneration system based on organic Rankine cycle installed with heat pumps. *Appl. Therm. Eng.* **2016**, *94*, 754–762. [CrossRef]
129. Sun, Y.; Lu, J.; Wang, J.; Li, T.; Li, Y.; Hou, Y.; Zhu, J. Performance improvement of two-stage serial organic Rankine cycle (TSORC) integrated with absorption refrigeration (AR) for geothermal power generation. *Geothermics* **2017**, *69*, 110–118. [CrossRef]
130. Ehyaei, M.A.; Ahmadi, A.; El Haj Assad, M.; Rosen, M.A. Investigation of an integrated system combining an Organic Rankine Cycle and absorption chiller driven by geothermal energy: Energy, exergy, and economic analyses and optimization. *J. Clean. Prod.* **2020**, *258*, 120780. [CrossRef]
131. Leveni, M.; Cozzolino, R. Energy, exergy, and cost comparison of Goswami cycle and cascade organic Rankine cycle/absorption chiller system for geothermal application. *Energy Convers. Manag.* **2021**, *227*, 113598. [CrossRef]
132. Wang, N.; Zhang, S.; Fei, Z.; Zhang, W.; Shao, L.; Sardari, F. Thermodynamic performance analysis a power and cooling generation system based on geothermal flash, organic Rankine cycles, and ejector refrigeration cycle; application of zeotropic mixtures. *Sustain. Energy Technol. Assess.* **2020**, *40*, 100749. [CrossRef]
133. Jafary, S.; Khalilarya, S.; Shawabkeh, A.; Wae-hayee, M.; Hashemian, M. A complete energetic and exergetic analysis of a solar powered trigeneration system with two novel organic Rankine cycle (ORC) configurations. *J. Clean. Prod.* **2021**, *281*, 124552. [CrossRef]
134. Jiménez-García, J.C.; Moreno-Cruz, I.; Rivera, W. Modeling of an Organic Rankine Cycle Integrated into a Double-Effect Absorption System for the Simultaneous Production of Power and Cooling. *Processes* **2023**, *11*, 667. [CrossRef]
135. Lizarte, R.; Palacios-Lorenzo, M.E.; Marcos, J.D. Parametric study of a novel organic Rankine cycle combined with a cascade refrigeration cycle (ORC-CRS) using natural refrigerants. *Appl. Therm. Eng.* **2017**, *127*, 378–389. [CrossRef]
136. Li, W.; Lin, X.; Cao, C.; Gong, Z.; Gao, Y. Organic Rankine Cycle-assisted ground source heat pump combisystem for space heating in cold regions. *Energy Convers. Manag.* **2018**, *165*, 195–205. [CrossRef]
137. Marty, F.; Serra, S.; Sochard, S.; Reneaume, J.M. Simultaneous optimization of the district heating network topology and the Organic Rankine Cycle sizing of a geothermal plant. *Energy* **2018**, *159*, 1060–1074. [CrossRef]
138. Maali, R.; Khir, T. Thermodynamic analysis and optimization of an ORC hybrid geothermal–solar power plant. *EuroMediterr. J. Environ. Integr.* **2023**, *8*, 341–352. [CrossRef]
139. Boukelia, T.E.; Arslan, O.; Djimli, S.; Kabar, Y. ORC fluids selection for a bottoming binary geothermal power plant integrated with a CSP plant. *Energy* **2023**, *265*, 126186. [CrossRef]
140. Javanshir, N.; Mahmoudi, S.M.S.; Rosen, M.A. Thermodynamic and Exergoeconomic Analyses of a Novel Combined Cycle Comprised of Vapor-Compression Refrigeration and Organic Rankine Cycles. *Sustainability* **2019**, *11*, 3374. [CrossRef]
141. Pashapour, M.; Jafarmadar, S.; Khalil Arya, S. Exergy Analysis of a Novel Combined System Consisting of a Gas Turbine, an Organic Rankine Cycle and an Absorption Chiller to Produce Power, Heat and Cold. *Int. J. Eng.* **2019**, *32*, 1320–1326. [CrossRef]
142. Sharifishourabi, M.; Arab Chadegani, E. Performance assessment of a new organic Rankine cycle based multi-generation system integrated with a triple effect absorption system. *Energy Convers. Manag.* **2017**, *150*, 787–799. [CrossRef]
143. Lee, H.; Ryu, B.; Anh, D.P.; Roh, G.; Lee, S.; Kang, H. Thermodynamic analysis and assessment of novel ORC- DEC integrated PEMFC system for liquid hydrogen fueled ship application. *Int. J. Hydrogen Energy Energy* **2023**, *48*, 3135–3153. [CrossRef]
144. Geng, D.; Du, Y.; Yang, R. Performance analysis of an organic Rankine cycle for a reverse osmosis desalination system using zeotropic mixtures. *Desalination* **2016**, *381*, 38–46. [CrossRef]
145. Wang, E.; Yu, Z.; Collings, P. Dynamic control strategy of a distillation system for a composition-adjustable organic Rankine cycle. *Energy* **2017**, *141*, 1038–1051. [CrossRef]
146. Gholamian, E.; Habibollahzade, A.; Zare, V. Development and multi-objective optimization of geothermal-based organic Rankine cycle integrated with thermoelectric generator and proton exchange membrane electrolyzer for power and hydrogen production. *Energy Convers. Manag.* **2018**, *174*, 112–125. [CrossRef]
147. Azad, A.; Fakhari, I.; Ahmadi, P.; Javani, N. Analysis and optimization of a fuel cell integrated with series two-stage organic Rankine cycle with zeotropic mixtures. *Int. J. Hydrogen Energy Energy* **2022**, *47*, 3449–3472. [CrossRef]
148. Kaşka, Ö.; Yılmaz, C.; Bor, O.; Tokgöz, N. The performance assessment of a combined organic Rankine-vapor compression refrigeration cycle aided hydrogen liquefaction. *Int. J. Hydrogen Energy Energy* **2018**, *43*, 20192–20202. [CrossRef]
149. Ganjehsarabi, H. Mixed refrigerant as working fluid in Organic Rankine Cycle for hydrogen production driven by geothermal energy. *Int. J. Hydrogen Energy Energy* **2019**, *44*, 18703–18711. [CrossRef]
150. Han, J.; Wang, X.; Xu, J.; Yi, N.; Ashraf Talesh, S.S. Thermodynamic analysis and optimization of an innovative geothermal-based organic Rankine cycle using zeotropic mixtures for power and hydrogen production. *Int. J. Hydrogen Energy Energy* **2020**, *45*, 8282–8299. [CrossRef]
151. Cao, Y.; Haghghi, M.A.; Shamsaiee, M.; Athari, H.; Ghaemi, M.; Rosen, M.A. Evaluation and optimization of a novel geothermal-driven hydrogen production system using an electrolyser fed by a two-stage organic Rankine cycle with different working fluids. *J. Energy Storage* **2020**, *32*, 101766. [CrossRef]

152. Fallah, M.; Mohammadi, Z.; Mahmoudi, S.M.S. Advanced exergy analysis of the combined S–CO2/ORC system. *Energy* **2022**, *241*, 122870. [CrossRef]
153. Wieland, C.; Schifflechner, C.; Braimakis, K.; Kaufmann, F.; Dawo, F.; Karellas, S.; Besagni, G.; Markides, C.N. Innovations for organic Rankine cycle power systems: Current trends and future perspectives. *Appl. Therm. Eng.* **2023**, *225*, 120201. [CrossRef]